同行专家业内评价意见书编号：20240858133

附件1

浙江工程师学院（浙江大学工程师学院）
同行专家业内评价意见书

姓名： 曾凡龙

学号： 22160125

申报工程师职称专业类别（领域）： 能源动力

浙江工程师学院（浙江大学工程师学院）制

2024年03月27日

一、个人申报

（一）基本情况【围绕《浙江工程师学院（浙江大学工程师学院）工程类专业学位研究生工程师职称评审参考指标》，结合该专业类别(领域)工程师职称评审相关标准，举例说明】

1.对本专业基础理论知识和专业技术知识掌握情况

本人本科期间就读于浙江大学能源工程学院机械设计制造及其自动化（汽车工程）专业，研究生阶段就读于浙江大学工程师学院车辆工程及其智能化项目，专业为能源动力。在知识掌握方面，具备较为扎实的数理基础，熟练掌握高等数学、工程图学、大学物理、理论力学、工程流体力学、工程热力学、传热学、内燃机学、汽车理论、优化算法等专业基础理论知识，英语水平通过CET-
6级考试。通过课程实践和工程实践，熟练掌握通过MATLAB/Simulink进行仿真建模、控制策略和算法搭建，掌握C、C++、Python等常用计算机语言，掌握通过vector
CANoe采集台架试验数据，在绘图上掌握autoCAD、Creo等工程实践中的常用软件。

2.工程实践的经历

工程实践方面，在重庆金康动力新能源有限公司进行了为期一年的校外专业实践项目，项目名为“新能源增程式混合动力控制系统研究”，主要研究内容为基于 MATLAB/Simulink
设计增程器控制器（RCU）控制策略，包含启停控制、增程器工作模式控制、增程器发电功率解耦下发、增程器发电功率反馈控制。通过各模块单元测试，以及结合被控对象模型的模型在环测试（MIL）验证增程器控制策略。在此过程中熟练掌握了基于MATLAB/Simulink进行车辆动力系统部件建模及验证的流程与方法。根据发动机、发电机与 RCU 之间的 CAN
通讯协议，明确控制策略模型的输入、输出接口，与 RCU 中间层软件接口保持一致，通过 Simulink 自动代码生成将控制策略烧录到 RCU
硬件，进一步通过硬件在环仿真（HIL）验证 RCU
功能及控制策略。在此过程中掌握了CAN总线相关的理论知识，掌握了对定义CAN报文的bdc文件的阅读能力，以及基于CANoe对CAN网络进行分析和数据采集的能力；同时通过对RCU中间层软件接口的定义锻炼了C语言实践能力。

3.在实际工作中综合运用所学知识解决复杂工程问题的案例

问题简介：需要利用动态规划算法（DP）求解给定车辆行驶车速曲线下，增程式电动汽车的最优能量管理策略。

问题难点：项目前期工作已实现通过DP求解未来5秒内最优车辆能量管理策略的算法，但目前需要对总行驶时间为30-
60分钟的整个行程进行最优能量管理策略求解，保证求解速度是关键难点。

具体解决过程：①车辆动力系统建模对求解精度和求解速度非常关键。通过增程器、动力电池、驱动电机等车辆动力总成主要部件的试验数据，构建了面向DP的动力系统简化静态模型：原方案中，动力电池开路电压、等效内阻的确定方式，是提前通过多项式拟合方法，从试验数据中获得开路电压、等效内阻关于动力电池荷电状态（SOC）的多项式计算公式。结合从《数值计算方法》课程所学的知识，多项式计算公式虽然拟合精度较高，但计算过程中需要多次乘法运算，总体计算效率不如离散点线性插值计算方法。于是将开路电压、等效内阻的确定方法从多项式计算改为离散点线性插值计算，在离散点间隔较小的情况下，这种简化造成的精度损失可以忽略不计。②在DP算法求解过程中，需要重复计算在特定状态点下执行特定控制量后，将要转移到的下一个状态点的位置，即状态转移计算。根据DP算法的原理，这样的计算一共会进行时间步数量×状态点数量×控制量数量次，然而所有状态点和控制量的组合一共仅有状态点数量×控制量数量种，因此存在大量重复计算。观察到这一点后，我选择预计算状态转移，提前将所有状态在所有控制量下的状态转移结果计算出来并保存在状态点数量×控制量数量大小的矩阵内，将复杂的状态转移计算简化为查表，遵循工程实践中常用的“以空间换时间”的思想，大大缩减了计算量。③在对原方案代码的阅读和反复试验

的过程中，通过对MATLAB的深入学习，了解到通过MATLAB记录工程中每个函数的调用次数和占用时间的方法，并由此发现原代码中较多使用了MATLAB的find()函数来实现在大矩阵中查找并提取符合条件的元素，而计算这一函数所花费的时间占用了总求解时间的93.8%。通过对MATLAB帮助文档的深入阅读和学习，认识到find()函数在大矩阵中使用时的严重弊端，并使用逻辑索引的方式代替find()函数，将总求解时间缩短了约90%。④结合应用的具体场景，对DP算法中的部分参数进行寻优，在保证精度的前提下缩短DP求解时间：考虑到本应用场景中，DP求解的对象为总行驶时间为30-
60分钟的总体为高速公路行驶场景下的行程，利用行业内的标准测试循环，构建了高速公路行驶场景下的测试循环，用于DP算法参数寻优。通过网格化搜索的方式，确定了最佳的状态量离散程度。
问题解决结果：在同样的软硬件平台下进行测试，测试工况为行驶时间约3000秒的行程。使用原算法对测试工况进行最优能量管理策略求解，求解花费时间将超过半个小时（1800秒）。使用优化后的算法，求解精度损失在1%以内，求解所需时间仅为6.5秒。通过对车辆动力系统适当的简化、对动态规划算法求解过程的优化、对MATLAB本身特性的细致研究和充分利用，大大减少了算法求解所需时间，基本解决了问题难点。

（二）取得的业绩（代表作）【限填3项，须提交证明原件（包括发表的论文、出版的著作、专利证书、获奖证书、科技项目立项文件或合同、企业证明等）供核实，并提供复印件一份】

1.
公开成果代表作【论文发表、专利成果、软件著作权、标准规范与行业工法制定、著作编写、科技成果获奖、学位论文等】

成果名称	成果类别 [含论文、授权专利（含发明专利申请）、软件著作权、标准、工法、著作、获奖、学位论文等]	发表时间/授权或申请时间等	刊物名称/专利授权或申请号等	本人排名/总人数	备注
基于动态规划的PHEV电池参考SOC规划研究	其他公开正式刊物	2024年10月28日	现代机械	1/1	
结合交通预测的PHEV电池SOC参考轨迹规划研究	会议论文	2023年11月12日	中国内燃机学会2023交通能源与智能动力大会	1/3	

2.其他代表作【主持或参与的课题研究项目、科技成果应用转化推广、企业技术难题解决方案、自主研发设计的产品或样机、技术报告、设计图纸、软课题研究报告、可行性研究报告、规划设计方案、施工或调试报告、工程实验、技术培训教材、推动行业发展中发挥的作用及取得的经济社会效益等】

（三）在校期间课程、专业实践训练及学位论文相关情况	
课程成绩情况	按课程学分核算的平均成绩： 86 分
专业实践训练时间及考核情况(具有三年及以上工作经历的不作要求)	累计时间： 1.5 年（要求1年及以上） 考核成绩： 85 分（要求80分及以上）
本人承诺	
个人声明：本人上述所填资料均为真实有效，如有虚假，愿承担一切责任，特此声明！ **申报人签名：**宿凡龙	

22160125

二、日常表现考核评价及申报材料审核公示结果

日常表现考核评价	非定向生由德育导师考核评价、定向生由所在工作单位考核评价： ☑优秀 ☐良好 ☐合格 ☐不合格 德育导师/定向生所在工作单位分管领导签字（公章）：　　年 3月27日
申报材料审核公示	根据评审条件，工程师学院已对申报人员进行材料审核（学位课程成绩、专业实践训练时间及考核、学位论文、代表作等情况），并将符合要求的申报材料在学院网站公示不少于5个工作日，具体公示结果如下： ☐通过 ☐不通过（具体原因：　　） 工程师学院教学管理办**公室**审核签字（公章）：　　年　月　日

浙 江 大 学 研 究 生 院

攻读硕士学位研究生成绩表

学号：22160125	姓名：曾凡龙	性别：男	学院：工程师学院	专业：能源动力	学制：2.5年
毕业时最低应获：26.0学分		已获得：27.0学分		入学年月：2021-09	毕业年月：2024-03
学位证书号：1033532024602165			毕业证书号：103351202402600391		授予学位：能源动力硕士

学习时间	课程名称	备注	学分	成绩	课程性质	学习时间	课程名称	备注	学分	成绩	课程性质
2021-2022学年秋季学期	学科前沿选论		2.0	88	专业学位课	2021-2022学年夏季学期	研究生英语基础技能		1.0	免修	公共学位课
2021-2022学年冬季学期	车辆信息传感与通信技术		2.0	90	专业学位课	2021-2022学年夏季学期	研究生英语		2.0	免修	公共学位课
2021-2022学年冬季学期	智慧能源系统工程		2.0	86	专业选修课	2021-2022学年春夏季学期	车辆工程专业课程设计与实践		4.0	84	专业学位课
2021-2022学年秋冬季学期	中国特色社会主义理论与实践研究		2.0	92	公共学位课	2021-2022学年夏季学期	工程伦理		2.0	92	公共学位课
2021-2022学年秋冬季学期	研究生论文写作指导		1.0	86	专业学位课	2021-2022学年春夏季学期	优化算法		3.0	96	专业选修课
2021-2022学年冬季学期	车辆控制理论与技术		3.0	89	专业学位课	2022-2023学年秋季学期	数值计算方法		2.0	93	专业选修课
2021-2022学年春季学期	自然辩证法概论		1.0	89	公共学位课						

说明：1. 研究生课程按三种方法计分：百分制，两级制（通过、不通过），五级制（优、良、中、及格、不及格）。

2. 备注中“*”表示重修课程。

学院成绩校核章：

成绩校核人：张梦依

打印日期：2024-04-02

代表作一

录用证明

《现代机械》版面费 ☆

发件人: **1123708596@qq.com** <1123708596@qq.com>

时　间: 2024年2月26日 (星期一) 上午10：21

收件人 **2455430281** <2455430281@qq.com>

附　件 1 个 (曾凡龙0024　录用通知书.doc)　　纯文本

《现代机械》交纳发表费通知

曾凡龙作者:

您撰写的文稿《基于动态规划的PHEV电池参考SOC规划研究》编号（2024.0024 ） 经专家定稿会审查同意刊登，并将在发表期间与您联系。如需刊登，请将发表费 1200 元，按照录用通知里的方式进行缴纳，并登录投稿系统系统填写相关费用信息、发票信息及邮寄地址等信息。如不按时完成上述内容将按撤稿处理。

《现代机械》编辑部

2024/2/26

附件(1 个)

普通附件 (已通过电脑管家云查杀引擎扫描)

曾凡龙0024 录用通知书.doc (25.78K)

预览　下载　收藏　翻译

论·文·录·用·通·知

曾凡龙·作者:·

·您于 2024 年 1 月向《现代机械》投稿，编号：2024—0024

题目:基于动态规划的 PHEV 电池参考 SOC 规划研究，经有关专家审定后可以在本刊发表。此稿暂定于 2024 年第 5 期(或 2024 年第 6 期）刊用，2024 年 10 月 28 日(或 2024 年 12 月 28 日)出刊；需交纳版面费 1200 元，版面费按最下方说明支付给编辑部。

请仔细阅读并谢谢您的合作。

联系电话:·0851-85951755·

http://xdjx.cbpt.cnki.net

《现代机械》编辑部

2024 年 2 月 26 日

代表作一
论文全文

基于动态规划的 PHEV 电池参考 SOC 规划研究

曾凡龙
（浙江大学 动力机械及车辆工程研究所，中国 杭州 310027）

摘要：合理的动力电池荷电状态（SOC）参考轨迹规划对于提高插电式混合动力汽车（PHEV）能量管理策略的优化性能非常重要。本研究提出了一种基于动态规划(DP)的参考 SOC 规划方法，从智慧交通系统（ITS）获取车辆未来经过不同路段时的交通流速度，进而通过 DP 进行参考 SOC 规划。通过参数寻优以及求解过程优化，改善了 DP 的求解时间。将所提出的 SOC 规划算法与自适应等效燃油消耗最小化策略（A-ECMS）相结合，使用真实世界数据的仿真结果表明，基于 DP 的参考 SOC 规划方法相比电量维持的参考 SOC，节省了 4.63%的综合燃油消耗量。

关键词：插电式混合动力汽车；能量管理策略；电池 SOC 参考轨迹；动态规划；
中图分类号：U469.72 文献标识码：A

Dynamic Programming-based PHEV Battery Reference SOC Planning

Fanlong Zeng
（Power Machinery and Vehicular Engineering Institute, Zhejiang University, Hangzhou, China, 310027）

Abstract: Battery state-of-charge (SOC) reference trajectory planning is very important to improve the performance of the plug-in hybrid electric vehicle (PHEV) energy management strategy. This paper proposed a SOC reference trajectory planning method based on dynamic programming, which obtains the traffic flow speed data of different road sections that the vehicle will pass through in the future from the intelligent transportation system (ITS), and then uses the dynamic programming (DP) algorithm to perform reference SOC planning. Through parameter optimization and solution process optimization, the solution time of DP is improved. Combining the proposed SOC planning algorithm with the adaptive equivalent fuel consumption minimization strategy (A-ECMS), simulation results using real-world data show that the DP-based reference SOC planning method saves 4.63% comprehensive fuel consumption than the charge-sustaining SOC reference.

Key words: Plug-in Hybrid Electric Vehicle; Energy Management Strategy; Reference SOC; Dynamic Programming

1 引言

能量管理策略（EMS）是插电式混合动力汽车（PHEV）的关键技术之一，合理的 EMS 能够通过对各动力源之间的能量分配，优化 PHEV 的动力性、经济性、动力电池寿命和 NVH 性能等。目前，以等效燃油消耗最小策略（ECMS）[1]和模型预测控制（MPC）为代表的基于实时优化的 EMS 受到广泛研究，由于 PHEV 的动力电池容量相对混合动力汽车（HEV）更大，电池荷电状态（SOC）能够在更大范围内变化，SOC 参考值的确定就成为基于实时优化的 EMS 必须要考虑的问题，也即参考 SOC 规划问题[2]。

针对 PHEV 的 EMS 中的 SOC 参考轨迹规划问题，国内外学者已开展了较多研究。智慧交通系统（ITS）的发展使车辆提前获取更多行程信息成为可能，Chao Sun 等[3]提出了结合实时交通速度数据的参考 SOC 规划算法，利用实时交通信息组成长时车速曲线，通过 DP 求解最优 SOC 参考轨迹，为下层基于 MPC 的 EMS 提供 SOC 参考值。基于行程信息的 SOC 参考轨迹规划能够充分利用实时交通信息，提高 EMS 的效果，但存在 DP 计算复杂度高、求解时间长等问题。

针对上述问题，本文设计了一种基于动态规划（DP）的 PHEV 电池参考 SOC 规划方法。通过 ITS 获得未来行驶路段的交通流速度，组成大致的未来行驶车速曲线，通过 DP 算法求解车速曲线对应的最优参考 SOC 轨迹。本文对 DP 的求解过程进行了优化，在保证求解精度的前提下减少了求解所需时间。最终通过仿真试验，将所规划的参考 SOC 用于 ECMS 能量管理策略，验证了所提出的基于 DP 的参考 SOC 规划方法。

2 全局车速的获取

美国加州高速公路性能评估系统（PeMS）通过部署在加州主要高速公路上的交通探测器，记录高速公路网各处的交通流量、交通速度等信息[4]，其中各路段的宏观交通流速度等信息能够实时获取，更新时间为 5 分钟。Mobile Century 数据集[5]通过移动电话的 GPS 功能采集了 2008 年 2 月 8 日加州 I-880 高速公路段上的 1388 条车辆的时空行驶轨迹数据，该路段的示意图如图 1（a）所示，图 1（b）展示了 PeMS 中该路段沿线交通探测器采集的宏观交通流速度信息。

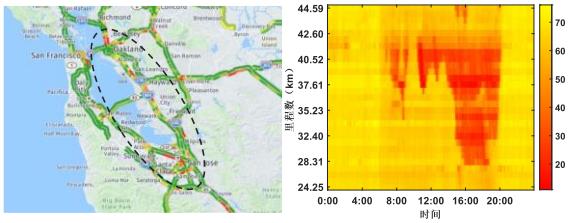

(a) (b)

图 1 Mobile Century 数据集采集区域及典型交通情况示意图

假设 Mobile Century 中采集的对象车辆在出发时通过 PeMS 准确获取到了后续路段的交通流速度信息，假设车辆未来行驶速度等于所在路段的交通流速度，通过三次埃尔米特插值，即可在出发时获得车辆大致的未来行驶车速曲线，如图 2 所示。

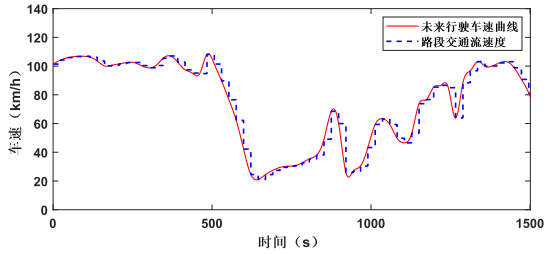

图 2 利用交通流速度得到未来行驶车速

从 Mobile Century 数据集中提取 10 条行驶轨迹，5 条一组拼接成两个较长的测试工况，用于对参考 SOC 规划方法的优化和验证，如图 3 所示。

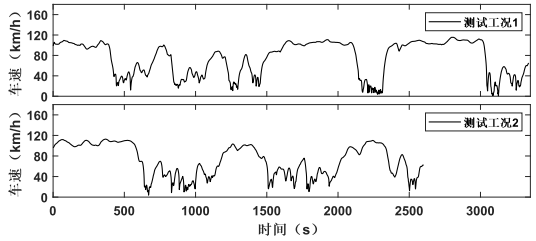

图 3 从 Mobile Century 数据集中提取的测试循环

3 基于动态规划的 SOC 规划

3.1 面向动态规划的 PHEV 动力系统简化模型

为利用 DP 进行参考 SOC 规划，首先建立面向 DP 的动力系统简化模型，本文的 PHEV 研究对象为某款增程式 SUV。

DP 的输入为行程的全局车速，DP 求解的离散时间步长为 1 秒。通过全局车速确定车辆每个时刻的整车需求功率，进而利用 DP 求解各个动力源的最佳能量分配。需求功率可由如下车辆纵向动力学公式计算：

$$P_{\mathrm{req}}(k)=\frac{v(k)}{3600\eta_{\mathrm{T}}\eta_{\mathrm{m}}}\cdot F_{\mathrm{t}}(k) \tag{1}$$

其中车辆行驶阻力F_{t}由下式计算：

$$F_{\mathrm{t}}(k)=\left(mgf\cos\alpha+mg\sin\alpha+\frac{C_D A v(k)^2}{21.15}+\delta m\frac{a(k)}{3.6}\right) \tag{2}$$

其中，k为当前离散时刻，s；v为车速，km/h；a为加速度，通过离散速度值做差分计算，$\mathrm{m/s^2}$；m为整车质量，kg；g 为重力加速度，$\mathrm{m/s^2}$；f为滚动阻力系数；α为坡度，°；C_{D}为风阻系数；A为迎风面积，$\mathrm{m^2}$；δ为旋转质量换算系数；η_{T}为传动系统的效率，%；η_{m}为驱动电机效率，%，通过驱动电机转速和转矩查表获得。驱动电机转速n_{Mot}、转矩T_{Mot}可通过车轮半径、传动系速比分别从车速和阻力矩换算得到：

$$n_{\mathrm{Mot}}=\frac{v(k)}{3.6r_{\mathrm{wheel}}}\cdot\frac{60}{2\pi}\cdot i_0 \tag{3}$$

$$T_{\mathrm{Mot}}=\frac{r_{\mathrm{wheel}}}{\eta_{\mathrm{T}}i_0}\cdot F_{\mathrm{t}}(k) \tag{4}$$

考虑整车的功率平衡，如图 4，忽略附件损耗，整车需求功率由增程器发电功率P_{RE}和电池功率P_{batt}提供。调整增程器工作点，可以改变P_{RE}的大小，由电池提供其余的需求功率。

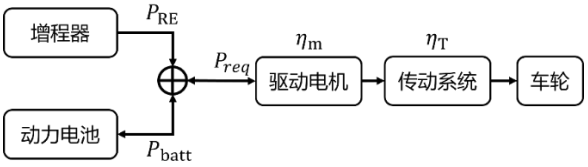

图 4 增程式电动汽车整车功率平衡示意图

于是动力系统的功率平衡如下式：

$$P_{\mathrm{req}}(k)=P_{\mathrm{batt}}(k)+P_{\mathrm{RE}}(k) \tag{5}$$

将增程器视作整体，不考虑增程器内部发动机与发电机的复杂动态过程，对增程器建立静态模型，假定增程器响应迅速、发电功率稳定。增程器高效发电运行曲线如图 5 所示，该运行曲线综合考虑了发动机万有特性和发电机效率、避开了共振区域以保证 NVH 性能，红色五角星标记的工作点是不同发电功率下所选取的最优工作点。

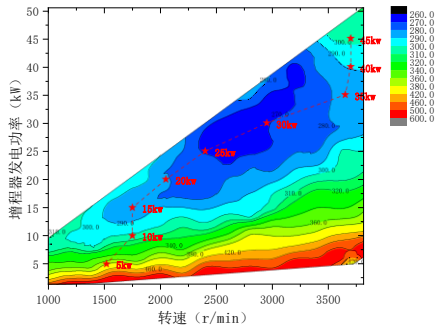

图 5 增程器油耗 map 及最优工作曲线

动力电池模型用一阶等效电路模型建模，其中动力电池的电流I_{batt}可由下式求得：

$$I_{\mathrm{batt}}(k)=\frac{U_{\mathrm{oc}}(k)-\sqrt{U_{\mathrm{oc}}(k)^2-4000\cdot R_{\mathrm{batt}}(k)\cdot P_{\mathrm{batt}}(k)}}{2R_{\mathrm{batt}}(k)} \quad (6)$$

其中U_{oc}为动力电池开路电压，V；R_{batt}为动力电池等效内阻，Ω。U_{oc}和R_{batt}在 23℃恒温下随 SOC 的变化关系通过电池芯充放电试验得到，如图 6 所示。

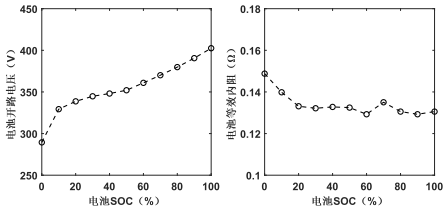

图 6 动力电池不同 SOC 下的开路电压及等效内阻

利用安时积分法估计电池 SOC 的变化率：

$$\dot{SOC}(k)=-\frac{I_{\mathrm{batt}}(k)}{3600\cdot Q_{\mathrm{b}}} \quad (7)$$

3.2 动态规划具体实现

选择电池 SOC 作为状态量，增程器发电功率P_{RE}作为控制量，增程器发电功率仅在图 5 中的有限个工作点中选取。联立（6）和（7），可以得到 DP 的状态转移方程。以最小化能量损耗作为 DP 规划参考 SOC 的优化目标；目标函数中还包含终点 SOC 约束项，以保证终点 SOC 到达目标 SOC。DP 单步损失函数和全局优化目标函数如下：

$$L(k,i,j)=\left(\dot{m}_{\mathrm{fuel}}(j)\cdot Q_{\mathrm{HV}}-P_{\mathrm{RE}}(j)\right)+I_{\mathrm{batt}}^2(i)\cdot R_{\mathrm{batt}}(i) \quad (8)$$

$$J_{\mathrm{DP}}=\min\left(\sum_{k=1}^{N}L(k,i,j)+\gamma\cdot(SOC_{\mathrm{end}}-SOC_{\mathrm{target}})^2\right) \quad (9)$$

其中SOC_{end}为终止时刻的 SOC 值；γ为终止 SOC 值偏离的惩罚项系数；$\dot{m}_{\mathrm{fuel}}(j)$为$k$阶段$j$控制量下的燃油消耗质量流量，kg/s；$Q_{\mathrm{HV}}$为汽油燃烧热值，46000kJ/kg。

在 DP 进行多阶段决策优化的过程中，整车被控对象的各个部件需要符合实际运行状态，因此需要考虑根据实际情况对各动力部件的关键参数进行如下约束：

$$SOC_{\min}\le SOC(k)\le SOC_{\max}$$

$$P_{\mathrm{batt,chg}}(SOC(k))\le P_{\mathrm{batt}}(k)\le P_{\mathrm{batt,dischg}}(SOC(k))$$

$$I_{\mathrm{batt,min}}(SOC(k))\le I_{\mathrm{batt}}(k)\le I_{\mathrm{batt,max}}(SOC(k))$$

$$P_{\mathrm{Mot,min}}\le P_{\mathrm{m}}(k)\le P_{\mathrm{Mot,max}}$$

$$T_{\mathrm{Mot,min}}(n_{\mathrm{Mot}}(k))\le T_{\mathrm{Mot}}(k)\le T_{\mathrm{Mot,max}}(n_{\mathrm{Mot}}(k))$$

其中$SOC_{\max}$和$SOC_{\min}$分别是动力电池 SOC 的上下限，%；$P_{\mathrm{batt,chg}}$和$P_{\mathrm{batt,dischg}}$分别是动力电池充放电功率的限制值，kW；$I_{\mathrm{batt,max}}$和$I_{\mathrm{batt,min}}$分别是动力电池充放电电流的上下限，A；$P_{\mathrm{Mot,max}}$和$P_{\mathrm{Mot,min}}$分别是驱动电机功率的上下限，kW；$T_{\mathrm{Mot,max}}$和$T_{\mathrm{Mot,min}}$分别是驱动电机扭矩的上下限，N·m；n_{Mot}为驱动电机转速，r/min。其中电池充放电功率限制、电池充放电电流限制均与 SOC 值相关，驱动电机的最大扭矩与其转速相关。

采用逆向求解的方式，根据以下迭代公式，从最终阶段往前推算每个阶段k、每个状态点i的最优子目标函数值$J^*(k,i)$：

对于 $k=N$:

$$J^*(k,i)=L_{\mathrm{SOC}}(SOC(i)) \quad (10)$$

对于 $1\le k<N$:

$$J^*(k,i)=\min_{0<j<N_a}\left(J^*(k+1,ii)+L(k,i,j)\right) \quad (11)$$

其中ii为第k阶段第i状态下采取第j控制量时将转移到的状态。对每个状态点，需要遍历其所有可能的控制量，找出使得子目标函数最小，且下一状态满足约束条件的最优控制量$P_{\mathrm{RE}}^*(k,i)$。由于状态量的离散化，给定控制量时，转移后的下一状态往往不能恰好落在网格点上，如图 7 所示。SOC_k^i代表第k阶段第i个状态点，当采取控制量u_j时，通过状态转移方程计算出其转移到SOC_{k+1}^{ii}状态，此 SOC 值介于SOC_{k+1}^{i1}和SOC_{k+1}^{i2}这两个状态点之间。采用线性插值的方式获得SOC_{k+1}^{ii}状态的子目标函数：

$$J_1=J^*(k+1,SOC_{k+1}^{i1}),\ J_2=J^*(k+1,SOC_{k+1}^{i2}) \quad (12)$$

$$J^*(k+1,SOC_{k+1}^{ii})=J_2+\frac{SOC_{k+1}^{ii}-SOC_{k+1}^{i2}}{\Delta SOC}(J_1-J_2) \quad (13)$$

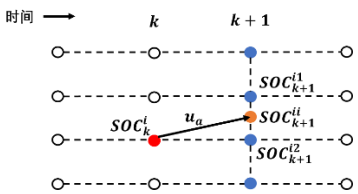

图 7 离散 SOC 网格下子目标函数插值示意图

逆向求解出状态空间内所有状态点的最优子目标函数之后，从初始 SOC 出发，正向推算出最优控制序列，其对应的电池 SOC 轨迹即为所求的参考 SOC 轨迹。DP 求解的算法流程图如图 8 所示。

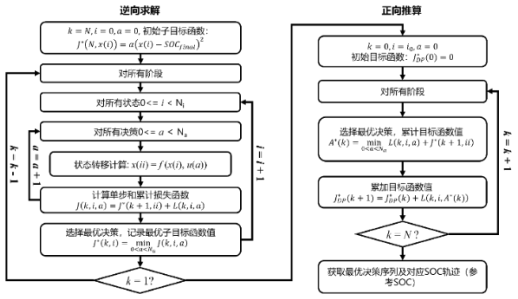

图 8 动态规划算法流程图

3.3 动态规划算法优化

3.3.1 状态量离散程度的确定

动态规划计算过程中，状态量离散程度直接影响求解精度和计算时间，若状态量即 SOC 的离散步长ΔSOC足够小，则求解精度较高，但计算时间更长。因此，有必要对ΔSOC进行寻优，达到计算精度与计算效率的折中。

以测试工况 1 作为试验工况，在初始 SOC 为 40%、目标 SOC 为 30%的条件下，试验 0.02，0.01，0.001，0.0001 四种ΔSOC下的 DP 求解情况。当ΔSOC大于 0.02 后，由于网格点过大，DP 算法无法求得有效解。表 1 展示了试验结果，随着网格点细化，计算时间线性增长，这是由于 DP 计算复杂度与状态点数量直接相关。以$\Delta SOC = 0.001$下的 SOC 轨迹为标准，计算各个情况下求解的 SOC 轨迹与标准 SOC 轨迹之间的最大误差。$\Delta SOC = 0.02$时，SOC 最大误差较为明显，终点 SOC 也已无法准确到达目标 SOC，油耗也高于其他情况。图 9 对比了这四种情况下求解得到的 SOC 轨迹，可见ΔSOC在0.01数量级以下时，DP 求解的 SOC 轨迹基本重合，缩小ΔSOC对求解精度的提升已经不明显。因此，选取$\Delta SOC = 0.01$。

表 1 不同ΔSOC下 DP 求解的结果

ΔSOC（%）	终点 SOC（%）	油耗（L）	计算时间（s）	SOC 最大误差（%）
0.02	29.98	3.938	12.22	0.164
0.01	30.00	3.937	29.73	0.081
0.005	30.00	3.936	65.92	0.041
0.001	30.00	3.936	388.91	/

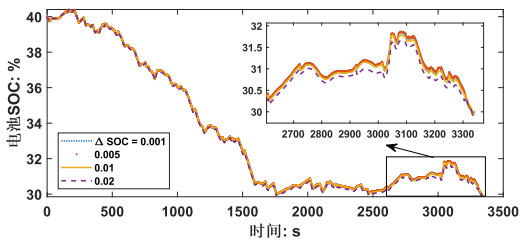

图 9 不同ΔSOC下 DP 求解的参考 SOC 结果

3.3.2 SOC 可行域限制

DP 求解所需时间与每个阶段的状态空间大小直接相关。由于电池的物理约束以及行程在每一阶段的需求功率固定，每一阶段中电池 SOC 的变化量有限，由此可以确定每一阶段 SOC 能够达到的最大范围，来减少需要遍历的状态点数量进而减少计算量，即 SOC 可行域限制。

由式（6）（7）可知，电池 SOC 变化率主要由电池充放电功率P_{batt}和当前 SOC 值决定，分别满足以下约束条件：

$$SOC_{\min} \le SOC(k) \le SOC_{\max} \quad (14)$$

$$P_{\mathrm{batt,chg}}(SOC(k)) \le P_{\mathrm{batt}}(k) \le P_{\mathrm{batt,dischg}}(SOC(k)) \quad (15)$$

对第k阶段，需求功率$P_{\mathrm{req}}(k)$可通过式（1）求得，根据增程器发电功率的上下限$P_{\mathrm{RE_max}}$和$P_{\mathrm{RE_min}}$，可以计算出电池功率的最大和最小值$P_{\mathrm{batt_high}}$和$P_{\mathrm{batt_low}}$：

$$P_{\mathrm{batt\_high}}(k) = \min\left(P_{\mathrm{batt,dischrg}}(k), P_{\mathrm{req}}(k) - P_{\mathrm{RE\_min}}\right) \quad (16)$$

$$P_{\mathrm{batt\_low}}(k) = \max\left(P_{\mathrm{batt,chrg}}(k), P_{\mathrm{req}}(k) - P_{\mathrm{RE\_max}}\right) \quad (17)$$

对于阶段k，其下一阶段$k+1$的 SOC 可行域上边界$SOC_{\mathrm{high}}(k+1)$和下边界$SOC_{\mathrm{low}}(k+1)$可以通过阶段k的 SOC 可行域边界推算得到，在k阶段$SOC_{\mathrm{high}}(k)$状态点处采取最小可行电池功率$P_{\mathrm{batt_low}}(k)$时，能够推算出 SOC 在下一阶段的 SOC 可行域上边界；在k阶段$SOC_{\mathrm{low}}(k)$状态点处采取最大可行电池功率$P_{\mathrm{batt_high}}(k)$时，则推算出 SOC 在下一阶段的 SOC 可行域下边界。如递推公式（18）和（19）所示，从初始阶段出发计算每个时刻的 SOC 可行域上下界，直至与式（14）中的 SOC 全局上下限重合。其中f_{Trans}为状态转移函数。

$$SOC_{\mathrm{high}}(k+1) = f_{\mathrm{Trans}}\left(SOC_{\mathrm{high}}(k), P_{\mathrm{batt\_low}}(k)\right) \quad (18)$$

$$SOC_{\mathrm{low}}(k+1) = f_{\mathrm{Trans}}\left(SOC_{\mathrm{low}}(k), P_{\mathrm{batt\_high}}(k)\right) \quad (19)$$

从终点时刻往前递推，可以进一步求解出从后往前的 SOC 可行域范围。与正向计算可行域时不同，逆向计算可行域时，需要把电池消耗P_{batt}功率后从阶段$k-1$到达阶段k的过程，等效为从阶段k消耗$-P_{\mathrm{batt}}$功率后到达阶段$k-1$。

在测试工况 1 上进行 SOC 可行域计算，SOC 的上限与下限分别为 100%和 20%。令初始 SOC 分别为 20%、40%、60%、80%，目标 SOC 为 30%。图 10 展示了初始 SOC 为 40%时的可行域示意图，其中深色区域代表 SOC 可行域，浅色区域代表被排除的不可行状态点，由图可知，通过上述 SOC 可行域限制方法，能够将不可行状态点排除在外，大大减少了 DP 算法需要搜索的状态空间。SOC 可行域计算结果如表 2 所示，SOC 可行域限制减少了 60%左右的状态点数量，缩短了 DP 求解时间。

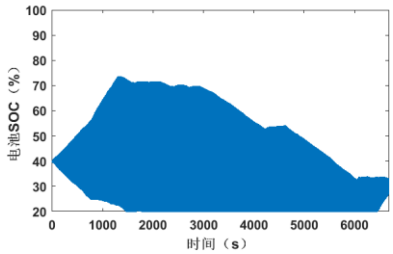

图 10 可行域限制后的 SOC 可行域示意图

表 2 SOC 可行域限制对状态点搜索空间的优化效果

初始 SOC	状态点数量（个）	状态点减少比例（%）
20	10236061	61.67
40	11192777	58.09
60	9470301	64.54
80	5536581	79.27

3.3.3 预计算状态转移矩阵和损失矩阵

注意到在 DP 求解过程中，需要频繁地计算状态转移函数以及单步损失函数，即：

$$SOC(k+1)=f_{\mathrm{Trans}}\left(SOC(k),P_{\mathrm{batt}}(k)\right) \tag{20}$$

$$L(k,i,a)=L_{\mathrm{batt}}\left(SOC(k),P_{\mathrm{batt}}(k)\right)+L_{\mathrm{RE}}\left(P_{\mathrm{RE}}(k)\right) \tag{21}$$

通过预计算状态转移结果以及单步损失结果并保存为状态转移矩阵和损失矩阵，以查表代替原计算过程，可以进一步减少 DP 求解时间。控制量P_{RE}只包含图 5 中的十个离散点，因此L_{RE}可通过一维查表获得；状态转移函数以及电池损失L_{batt}均只和 SOC 值以及电池功率P_{batt}有关。构建状态转移矩阵$\boldsymbol{\mathcal{T}}_{\mathrm{batt}}\in\mathbb{R}^{N_S\times N_A}$和损失矩阵$\boldsymbol{\mathcal{R}}_{\mathrm{batt}}\in\mathbb{R}^{N_S\times N_A}$，其中$N_S$和$N_A$分别表示 SOC 和$P_{\mathrm{batt}}$的离散点数量，矩阵中的元素满足：

$$\boldsymbol{\mathcal{T}}_{\mathrm{batt}}(i,j)=f_{\mathrm{Trans}}\left(SOC(i),P_{\mathrm{batt}}(j)\right) \tag{22}$$

$$\boldsymbol{\mathcal{R}}_{\mathrm{batt}}(i,j)=L_{\mathrm{batt}}\left(SOC(i),P_{\mathrm{batt}}(j)\right) \tag{23}$$

SOC 和P_{batt}的离散引入了误差，离散程度越细化，误差越小。然而矩阵存储需要额外空间，且矩阵大小对于内存访问速度也有影响，因此，需要对离散程度进行寻优。SOC 的离散程度在上文已确定，因此对P_{batt}的最优离散步长ΔP_{batt}进行参数优化，平衡求解精度和计算时间。

在测试工况 1 下进行仿真试验，设置初始 SOC 为 40%、目标 SOC 为 30%，对ΔP_{batt}为 0.01kW，0.1kW，1kW，2kW 这几种情况进行试验，并与没有通过查表简化的原始 DP 的结果进行对比，结果如表 3 所示。可以看出，ΔP_{batt}增加到 0.1 以后，计算时间显著下降。ΔP_{batt}的进一步增大没有显著减少计算时间，但显著增大了 DP 求解的误差。图 11 展示了各种ΔP_{batt}值下的 SOC 轨迹对比。可以看出，当ΔP_{batt}=2kW 时，由于$\boldsymbol{\mathcal{T}}_{\mathrm{batt}}$和$\boldsymbol{\mathcal{R}}_{\mathrm{batt}}$的离散网格太大，DP 计算各状态最优子目标函数时引入了过多的误差，已经严重偏离最优解。综合计算精度和计算时间，选择ΔP_{batt}=0.1kW 作为最终的状态转移矩阵和损失矩阵的电池功率离散步长。由表 3 的结果可以看出，通过预计算状态转移矩阵和损失矩阵，相比原 DP 算法缩短了 22.75%的计算时间。

表 3 不同ΔP_{batt}下 DP 求解的结果

ΔP_{batt}（kW）	终止 SOC（%）	油耗（L）	计算时间（s）	最大 SOC 误差(%)
原 DP	30.00	3.937	11.91	/
0.01	30.00	3.937	10.78	0
0.1	30.00	3.937	9.20	0.041
1	30.00	3.937	8.18	0.205
2	30.00	3.945	7.99	1.992

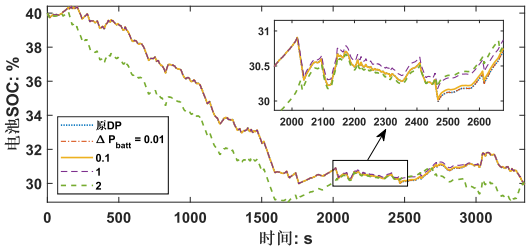

图 11 不同ΔP_{batt}下 DP 求解的参考 SOC 结果

从表 1 可知，DP 在优化求解过程前，在测试工况下的计算时间为 17.91 秒，表 3 表明优化求解过程后，计算时间缩短到了原来的 25.15%，对于长约 3400 秒的测试工况，计算时间为 9.20 秒。文献[3]中同样基于简化动力模型利用 DP 在线规划参考 SOC，在总长度 3500 秒左右的驾驶工况下，计算时间约为 30 秒。由此可见，本文所提出的参考 SOC 规划算法在计算时间方面能够满足在线应用的需求。

3.4 参考 SOC 结果输出

通过 DP 求解得到参考 SOC 与时间的对应关系曲线（SOC-t）。文献[3,6]中通过对比得出结论，根据行驶里程获取参考 SOC 值相比基于行驶时间获取参考 SOC 值的效果更好，因为实际行驶条件下通常总行驶里程固定，而总驾驶时间会随交通情况变化而波动较大。通过全局车速曲线，积分获得累积行驶路程序列$\boldsymbol{S}_{\mathrm{acc}}=\{S_1,S_2\ldots S_T\}$，将参考 SOC 曲线的横坐标替换为$\boldsymbol{S}_{\mathrm{acc}}$并执行样条曲线插值，获得最终的参考 SOC 输出（SOC-S），如图 12 所示。

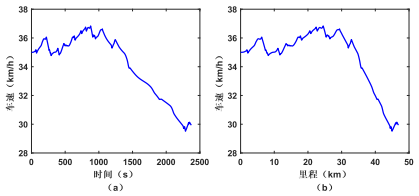

图 12 参考 SOC 结果。（a）SOC-t 曲线；（b）SOC-S 曲线

参考 SOC 规划完成后，保存在控制器中，行驶时依据当前已行驶里程，查取对应的参考 SOC 值。

4 仿真试验验证

4.1 结合能量管理策略的 SOC 规划验证

基于增程式电动汽车前向仿真平台进行仿真试验，将所规划的参考 SOC 用于能量管理，验证所提出的基于 DP 的参考 SOC 规划方法。仿真平台如图 13 所示。仿真平台在 MATLAB/Simulink 建立，模型各主要部件的参数信息及所涉及的主要控制策略均在之前的工作中有详细陈述[7]。将所规划的参考 SOC 用于自适应等效燃油消耗最小化策略（A-ECMS），来评估参考 SOC 的效果。A-ECMS 根据电池实际 SOC 与参考 SOC 的偏差自适应调整等效因子，能够较为准确地实现对参考 SOC 的跟踪[7]。

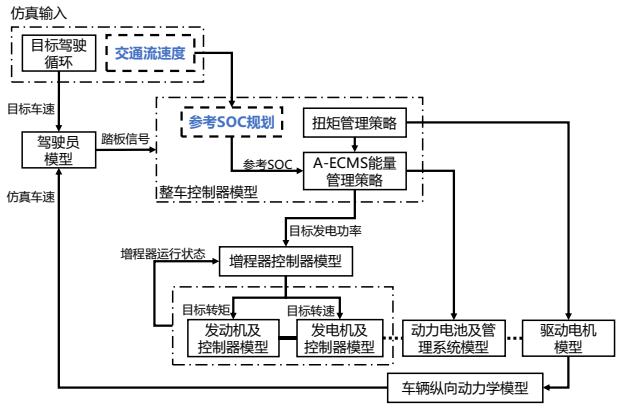

图 13 整车前向仿真平台示意图

进行以下几组仿真来评估所提出的参考 SOC 规划方法的效果。

1）DP：在对整个行程的行驶工况完全已知的情况下，通过 DP 计算出的能量管理全局最优解。

2）CS-ECMS：以纯电模式行驶直到 SOC 下降到预设阈值（30%）以下，然后启动 A-ECMS 进入电量维持模式（参考 SOC 值固定）。

3）DP-ECMS：A-ECMS 应用本文所提出的基于 DP 的参考 SOC。

4.2 仿真试验

图 14 和图 15 分别展示了三种 EMS 在初始 SOC 为 40%时的电池 SOC 变化曲线以及增程器工作点变化情况，表 4 列出了主要仿真指标的结果，其中综合燃油消耗量修正了终点 SOC 对应电耗的等效油耗，消除了不同 EMS 策略下终点 SOC 不同带来的油耗差别。

从图 14 可以看出，利用 DP 规划出的参考 SOC 能够指导 A-ECMS 达到接近全局最优解的 SOC 变化曲线。从图 15 可以看出，DP-ECMS 与 DP 全局最优解在增程器工作时机上较为一致。而电量维持的 CS-ECMS 先消耗完电能再保持电量维持，与 DP 全局最优差距较大。从数值结果来看，DP-ECMS 相比 CS-ECMS，减少了 4.63%的综合燃油消耗量。

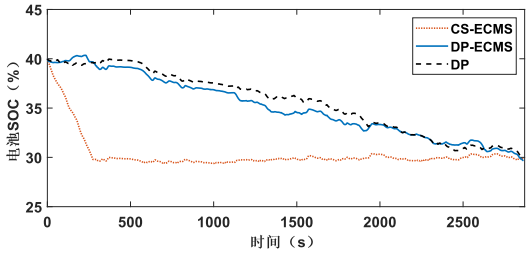

图 14 测试工况 2 下不同 EMS 的 SOC 变化情况

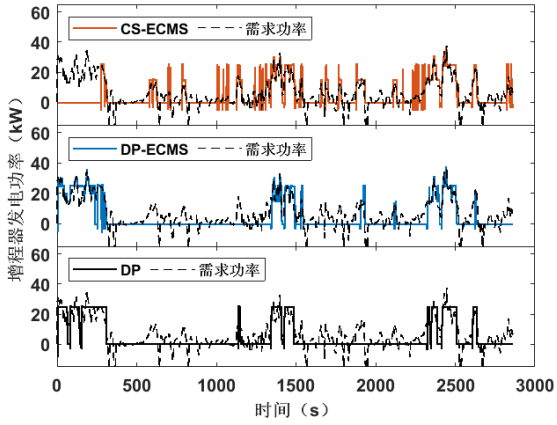

图 15 测试工况 2 下不同 EMS 的增程器工作点变化情况

表 4 测试工况 2 下应用不同参考 SOC 的仿真结果

组别	终点 SOC（%）	增程器启动次数	综合燃油消耗量（L）	百公里综合油耗（L）
CS-ECMS	29.79	45	1.582	3.779
TP-ECMS	29.66	15	1.509	3.604
全局最优	29.96	10	1.488	3.556

5 结论

针对 PHEV 的参考 SOC 规划问题，提出了一种基于 DP 的参考 SOC 规划方法。通过参数寻优以及对求解过程优化，优化了 DP 的计算时间，解决了 DP 算法计算量大、难以实时应用的问题。将所提出的参考 SOC 规划方法与 A-ECMS 能量管理策略结合，使用真实世界数据的仿真结果表明，基于 DP 规划的参考 SOC 相比电量维持的参考 SOC，减少了 4.63%的综合油耗，有效改善了燃油经济性。

参考文献

[1] Yao M, Zhu B, Zhang N. Adaptive Real-Time Optimal Control for Energy Management Strategy of Extended Range Electric Vehicle[J]. Energy Conversion and Management, 2021, 234: 113874.

[2] Zhang X, Guo L, Guo N, et al. Bi-Level Energy Management of Plug-in Hybrid Electric Vehicles for Fuel

Economy and Battery Lifetime with Intelligent State-of-Charge Reference[J]. Journal of Power Sources, 2021, 481: 228798.

[3] Chao Sun, Moura S J, Xiaosong Hu, et al. Dynamic Traffic Feedback Data Enabled Energy Management in Plug-in Hybrid Electric Vehicles[J]. IEEE Transactions on Control Systems Technology, 2015, 23(3): 1075–1086.

[4] Chen C, Petty K, Skabardonis A, et al. Freeway Performance Measurement System: Mining Loop Detector Data[J]. Transportation Research Record: Journal of the Transportation Research Board, 2001, 1748(1): 96–102.

[5] Herrera J C, Work D B, Herring R, et al. Evaluation of Traffic Data Obtained via GPS-Enabled Mobile Phones: The Mobile Century Field Experiment[J]. Transportation Research Part C: Emerging Technologies, 2010, 18(4): 568–583.

[6] Wei X, Wang J, Sun C, et al. Guided Control for Plug-in Fuel Cell Hybrid Electric Vehicles via Vehicle to Traffic Communication[J]. Energy, 2023, 267: 126469.

[7] Yao D, Lu X, Chao X, et al. Adaptive Equivalent Fuel Consumption Minimization Based Energy Management Strategy for Extended-Range Electric Vehicle[J]. Sustainability, 2023, 15(5): 4607.

作者简介：曾凡龙（2000－），男，四川内江人，硕士研究生，研究方向：混合动力汽车能量管理策略。

代表作2
会议论文录用及获奖证书

中国内燃机学会
CHINESE SOCIETY FOR INTERNAL COMBUSTION ENGINES

2023交通能源与智能动力大会

2023 CONFERENCE ON TRANSPORTATION ENERGY AND INTELLIGENT POWER (TEIP)

优秀论文证书

BEST PAPER CERTIFICATE

曾凡龙、姚栋伟、吴锋

撰写的

《结合交通预测的PHEV电池SOC参考轨迹规划研究》

被大会录用并评为优秀论文

中国内燃机学会

2023年11月12日

代表作2
论文全文

交通能源与智能动力大会
Conference on Transportation Energy and Intelligent Power

结合交通预测的 PHEV 电池 SOC 参考轨迹规划研究

曾凡龙[1]，姚栋伟[1,2]，吴锋[1]
（1.浙江大学 动力机械及车辆工程研究所，杭州 310027；2.浙江省汽车智能热管理科学与技术重点实验室，台州 317200）

Traffic Prediction Based Battery State of Charge Planning for Plug-in Hybrid Electric Vehicle

Fanlong Zeng[1], Dongwei Yao[1,2], Feng Wu[1]
(1.Power Machinery and Vehicular Engineering Institute, Zhejiang University, Hangzhou 310027 China a; 2. Key Laboratory of Smart Thermal Management Science & Technology for Vehicles of Zhejiang Province, Taizhou 317200, China)

Abstract: Battery state-of-charge (SOC) planning utilizing traffic information from the intelligent transportation system (ITS) and the Internet of Vehicles is promising to improve the performance of the connected plug-in hybrid electric vehicle (PHEV) energy management strategy. In this paper, a novel SOC reference trajectory planning method based on traffic forecast was proposed. A data-driven spatio-temporal graph convolutional neural network (STGCN) model was trained to predict the traffic speed of road networks. Thus, the long-term global speed profile can be predicted. Then a DP-oriented simplified power balance model was established and the global reference SOC trajectory was planned through dynamic programming (DP) algorithm. Finally, the proposed SOC planning algorithm was combined with an adaptive equivalent consumption minimization strategy (A-ECMS) and verified through simulation. Simulation results using real world traffic data illustrate that the proposed reference SOC planning method saves 1.76% and 2.27% of fuel consumption respectively compared with the charge sustaining reference SOC and the linear decrease reference SOC.

摘 要: 合理的动力电池荷电状态（SOC）规划对于提高插电式混合动力汽车（PHEV）能量管理策略的性能非常重要。本研究提出了一种基于交通预测的 SOC 参考轨迹规划方法，基于历史交通信息，使用数据驱动的时空图卷积神经网络（STGCN）模型来预测道路网络的交通速度，在此基础上预测全局车速曲线。建立了面向动态规划（DP）的简化功率平衡模型，通过 DP 算法，利用预测的全局车速曲线规划 SOC 参考轨迹。最后，将所提出的 SOC 规划算法与自适应等效消耗最小化策略（A-ECMS）相结合，使用真实交通数据的仿真结果表明，与电量维持的参考 SOC 和线性变化的参考 SOC 相比，所提出的参考 SOC 规划方法分别节省了 1.76%和 2.27%的燃料消耗。

关键词: 插电式混合动力汽车；能量管理策略；电池 SOC 参考轨迹；交通预测；
Key words: plug-in hybrid electric vehicle; energy management strategy; reference SOC; traffic forecast
中图分类号: TK402（请查阅中图分类法第 5 版）　　**文献标识码:** A

0 Introduction

The plug-in hybrid electric vehicle (PHEV) has multiple energy sources, which makes it more potential in energy saving and emission reduction, and it has no range anxiety of pure electric vehicles, thus its related technologies have received extensive attention[1].A PHEV generally contains multiple power sources, and the combination of multiple energy sources can effectively avoid the inefficient working area of a single energy source, helping to increase the life of the energy source and reduce system energy loss[2]. But at the same time, the power allocation problem of PHEV multi-energy sources is a typical multi-objective, multi-constraint and strongly nonlinear optimization problem, which is a difficult issue in the control of PHEV.

In order to ensure the vehicles' power performance, fuel economy, battery life and the noise, vibration and harshness (NVH) performance of PHEV, an efficient and reasonable energy management strategy (EMS) is required[3]. According to the optimization methods used, EMS is mainly divided into three categories[4]: rule-based methods, global optimization-based methods, and instantaneous optimization-based methods.

The global optimization-based EMS can achieve global optimum effects. However, full knowledge of the trip in advance and powerful computing power is a must. Due to the dynamically changing traffic environment, the full trip information of vehicles driving on open roads cannot be obtained in advance, so global optimization-based EMS is difficult for practical application. Instantaneous optimization based on partial trip information can not only realize online application, but also has a better optimization effect than rule-based methods. Among them, the equivalent fuel consumption minimization strategy (ECMS)[5] and the model predictive control (MPC)-based predictive energy management strategy (PEMS)[6] are the two most widely studied EMSs based on instantaneous optimization. Since the power battery capacity of PHEV is larger than that of non-plug-in hybrid electric vehicle (HEV), the battery SOC of PHEV can change in a wide range. So how to determine the target SOC is a problem must be considered when solving the optimization problem online, that is, the reference SOC planning problem.[7]

Many researches have been carried out aiming at the problem of reference SOC planning in the EMS of PHEV. Liu Y et al.[8] applied PEMS in which the SOC reference trajectory decreased linearly according to the driving distance on a fuel cell extended-range electric vehicle, and the reference SOC value was determined at the end of the rolling optimization prediction time according to the ratio of the remaining distance of trip to the full distance. Considering that in the actual driving cycle, the required power of the vehicle from the start to the end is usually not uniformly distributed, the assumption of a linear decrease in SOC is not reasonable. Zhou Q et al.[9] used the predicted short-term vehicle speed sequence, the driving distance, and the current driving speed and acceleration as the inputs of artificial neural network to forecast the reference SOC. This data-driven reference SOC determination method can be applied online, but its accuracy heavily depends on the training data.[10] The development of intelligent transportation system (ITS) has made it possible for vehicles to obtain more travel information in advance. Chao Sun et al.[11] proposed a SOC reference trajectory planning algorithm combined with real-time traffic speed data, using real-time traffic information to form a long-term vehicle speed curve, utilizing dynamic programming (DP) to obtain the optimal reference SOC trajectory to provide reference SOC value for the lower layer of MPC-based EMS. Reference SOC planning based on traffic information can make full use of the real-time traffic information, but it did not take into account the dynamic changes of traffic conditions over time, and the calculation consumption of dynamically updating SOC reference trajectory planning is too large.

In view of the above problems, this paper designed a PHEV battery SOC reference trajectory planning method combined with traffic forecasting. First, a data-driven traffic prediction model based on spatio-temporal graph convolutional neural network was built and validated. Then the future long-term speed profile was predicted using traffic forecasting results. With the predicted global speed profile, through DP algorithm, the optimal reference SOC trajectory was generated. Finally, through simulation performed on a range-extender electric vehicle(REEV) forward simulation platform, the reference SOC planning method was verified. By combing the proposed reference SOC with an adaptive ECMS(A-ECMS) energy management strategy in simulation , the performance of A-ECMS was improved compared with the linearly declining reference SOC trajectory. Thus the proposed reference SOC planning algorithm was further verified.

The rest of this paper is organized as follows. Section II introduces the traffic prediction-based long-term speed prediction. Section III introduces the proposed DP-based reference SOC planning method. Section IV presents the simulation and discussions of the proposed method, and the effect of the reference SOC planning on EMS. Section V summarizes the main conclusions.

1 Traffic Based Long-term Speed Prediction

In future practical applications, the traffic forecast data is assumed to be processed by the ITS in the cloud, the vehicle only needs to acquire the traffic forecast data of each node along its route through the cloud for long-term vehicle speed generation. As shown in Fig. 1, the navigation system on the vehicle plans the driving route on departure. According to the driving route, the traffic detectors that locate along the route are known. The ITS continuously collects traffic data from the road network through traffic detectors and stores the data in database. At the same time, through graph neural network(GNN) based traffic forecast model, the road network can be treated as a whole, which brings convenience in predicting the future traffic condition of all road sections that equipped with the traffic detectors at one time. This also helps long-term vehicle speed prediction in that regardless of the start point, end point, and driving route, as long as the vehicle drives within the given road network range, the future traffic conditions along the route can be known according to the predicted traffic information of the traffic detectors along the route, which can be obtained from ITS.

In this study, in order to explore the possibility of traffic forecasting to improve the effect of SOC planning, a traffic forecasting model was trained and validated to provide traffic prediction data. Then a long-term vehicle speed generation method based on traffic forecasting was designed to predict the global driving condition.

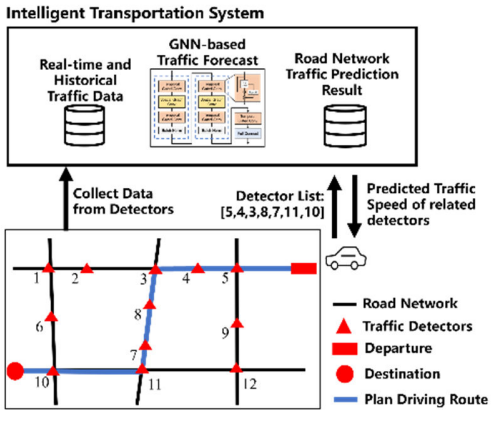

Fig. 1. Schematic diagram of vehicle acquiring data from ITS

1.1 Traffic Speed Prediction

Short-term traffic forecasting is an important research topic in transportation engineering field[12]. According to the

algorithm used, traffic forecast method can be divided into traditional statistics-based methods and neural network-based methods[13]. Traffic prediction problem within road networks usually require simultaneous processing of information collected by multiple traffic detectors distributed in different locations. The future traffic condition is not only related to the past historical information in time, but also has a certain correlation with the traffic conditions between different nodes in space. Because traditional statistical based methods are difficult to deal with traffic data that includes both time-dependency and space-dependency, spatio-temporal graph convolutional neural network (STGCN)[14] is applied to build a short-term traffic speed prediction model.

Traffic data of a road network is represented in graph structure. As shown in Fig. 2, the nodes in graph indicate the traffic detectors with traffic data while the set of edges indicates the connectedness between stations. Traffic data at time t can be expressed as $\mathbf{X}_t = (\mathbf{x}_{1,t}, \mathbf{x}_{2,t}, \dots, \mathbf{x}_{N,t})^T \in \mathbb{R}^{N\times C}$, where $\mathbf{x}_{i,t} \in \mathbb{R}^C$ represents the traffic data of the i-th node at time t, N is the number of traffic detector nodes, and C is the number of different types of features in the traffic data. Then the historical traffic data in the past time window of length h can be expressed as $\mathcal{X} = (\mathbf{X}_{t-h+1}, \mathbf{X}_{t-h+2}, \dots, \mathbf{X}_t) \in \mathbb{R}^{N\times C\times h}$. The spatial interdependence of traffic detector nodes can be represented by the adjacency matrix $W \in \mathbb{R}^{N\times N}$. According to the usage scenarios and goals, there are many ways to construct the adjacency matrix [15]. In the application scenario of this paper, the number of traffic nodes is less in quantity and the connection relationship is not complicated. Thus the adjacency matrix is constructed in the following form:

$$w_{ij} = \begin{cases} 1, \text{ if } i \text{ connect with } j \\ 0, \text{ otherwise} \end{cases} \tag{1}$$

where i and j are the indexes of two traffic detector nodes, and the order of the row index and column index in W is consistent with the order of the detector nodes of $\mathcal{X}$.

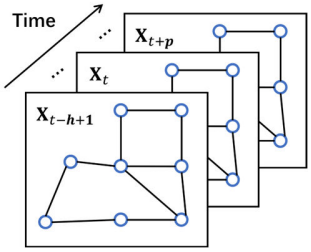

Fig. 2. Graph-structured traffic data.

Thus the training process of short-term traffic forecast model can be expressed as :

$$\min_{W_\theta} g(\mathcal{Y}, \hat{\mathcal{Y}}) \tag{2}$$

$$\hat{\mathcal{Y}} = f(\mathcal{X}; W_\theta) \tag{3}$$

where function f represents the traffic prediction model, and W_θ represents the parameters to be trained in the model. The model takes the historical traffic information $\mathcal{X}$ as input, and outputs the traffic prediction result $\hat{\mathcal{Y}} \in \mathbb{R}^{N\times C\times p}$ in the forecast time window of length p in the future. $\mathcal{Y}$ represents the ground truth traffic speed in the corresponding forecast time window. The function g represents the objective function used to optimize the traffic prediction model, where mean square error (MSE) is usually used:

$$g(\mathcal{Y}, \hat{\mathcal{Y}}) = \frac{\sum_{i=0}^{n}(y_i - \hat{y}_i)^2}{n} \tag{4}$$

where n is the number of samples in training set, y_i and $\hat{y}_i$ denotes the sample and label of traffic prediction dataset, respectively.

Fig. 3 presents the structural diagram of the STGCN-based traffic prediction model used. It mainly consists of several spatial graph convolution modules and temporal convolution modules. The spatial graph convolution module extracts spatial features in the traffic data using Chebyshev polynomial approximation of graph convolution:

$$\Theta *_{\mathcal{G}} x = \Theta(L)x \approx \sum_{k=0}^{K-1} \theta_k T_k\left(\tilde{L}\right) x \tag{5}$$

where Θ is the parameters of the graph convolution kernel, $*_{\mathcal{G}}$ is the graph convolution operator, x is the traffic data tensor in the graph structure, L is the normalized graph Laplacian matrix calculated by the adjacency matrix W, K is the size of the graph convolution kernel, $\theta \in \mathbb{R}^K$ is the coefficients of the Chebyshev polynomial, $T_k(\tilde{L})$ is the Chebyshev polynomial of order k evaluated at the scaled Laplacian $\tilde{L}$.

The temporal convolution module uses 1-D causal convolution with gated linear unit (GLU) activation function to extract temporal features in the graph structure. The structure of GLU is shown in the upper right corner of Fig. 3. Temporal convolution and spatial graph convolution are performed alternately, and the size of channels are 64 and 16, respectively. The batch normalization (BN)[16] layer can deal with the distribution change between different samples in a small batch, and improve the training efficiency and training effect in deep network.

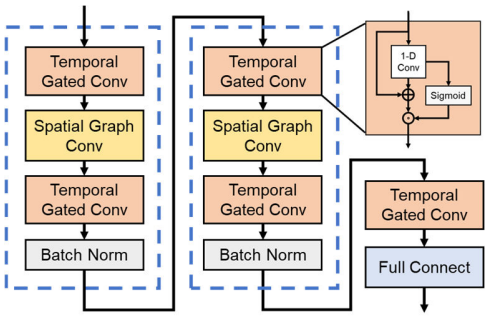

Fig. 3. Architecture of spatio-temporal graph neural network

1.2 Validation of Traffic Speed Prediction Model

Real-world traffic datasets were used to verify the traffic speed prediction model. Performance Measurement System (PeMS)[17] project conducted by California Department of Transportation records information such as traffic flow and traffic speed throughout the California highway network through traffic detectors deployed on highways. Different time and area of its data was produced as multiple public datasets

(PeMS04, PeMS08, etc.), which were widely used in the field of short-term traffic prediction. Mobile Century dataset was established by UC Berkeley and Nokia through experiments[18], which contains the spatio-temporal trajectory data of 1388 vehicles on the California I-880 road section on February 8, 2008. The combination of those two datasets was constructed in this paper for the verification of traffic prediction method as well as long-term speed generation method that will be described in detail in next chapter.

According to the roads involved in the Mobile Century dataset, a total of 28 traffic detectors with an absolute mileage from 16.4 miles to 27.7 miles in the northbound direction of the I-880 highway in PeMS were selected as the dataset for the traffic prediction algorithm. The selected road network area and corresponding traffic speed on a typical weekday are shown in Fig. 4. The selected time period was the working days from February 2007 to February 2008. By comparison, it was found that the recent traffic situation in this area was still almost the same as that in 2008[19], so this dataset is not outdated for study. The traffic data were aggregated every 5 minutes. The training set, validation set, and test set were divided according to the ratio of 3:1:1 in strict time order. The traffic dataset was denoted as PeMS-MC. It is worth mentioning that February 8, 2008, which is the exact day on which Mobile Century dataset was collected, was divided into the test set of PeMS-MC.

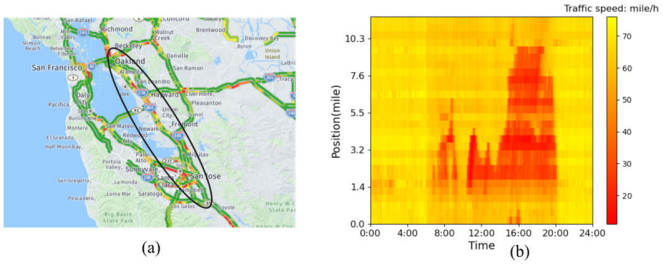

Fig. 4. Information of traffic prediction target area. (a) Road network in PeMS I880-N area. (b) Traffic speed thermal map of the area on a typical weekday.

The traffic prediction model was deployed on Windows 11 operating system based on the PyTorch framework, using CUDA hardware acceleration (CPU: Intel(R) Core(TM) i7-12700H@2.30 GHz, GPU: NVIDIA GeForce RTX 3050Ti Laptop GPU, 16GB RAM). The input time window of the model was the past 60 minutes, that is, 12 historical observation data points, and the output was the average vehicle speed of the road section in the next 15, 30, and 45 minutes. Due to the limitation of the model itself, the long-term traffic prediction effect of more than 45 minutes was not stable, therefore only time points within 45 minutes were considered. The learning rate was set to 10^{-3}. The hyperparameters of the model were determined through grid search, and the number of samples in a mini-batch was set to 64. The early stopping mechanism was used in the training process, and the mean square error(MSE) evaluated on the validation set was used as the evaluation index for early stopping. The maximum allowable epochs of early stopping is set to 5 rounds, that is, if the MSE evaluated on validation set had no further decline after 5 epochs of training, the training was stopped and the epoch with lowest validation MSE was selected as final model.

Error metrics Mean Absolute Error(MAE), Root Mean Square Error (RMSE), Mean Absolute Percentage Error (MAPE) were used as performance metrics to measure and evaluate the performance of different methods. The following baseline models are used for comparison with the STGCN traffic prediction model applied in this paper: 1) Historical average method (HA): The historical average traffic speed at the same time-of-the-day in the past week in the dataset is used as the predicted value. 2) No prediction method (NM, Naive Method), that is, the traffic data at the latest moment is used as the prediction value for the future. 3) Back Propagation Neural Network (BPNN): Two hidden layers, 1000 neurons in each layer. Dropout method with dropout probability of 50% was applied on both layers to avoid overfitting. 4) Convolutional Neural Network (CNN): Refer to the model in [13]. The prediction performance of various models on the test data set are shown in TABLE I.

TABLE I. shows that the model built in this paper based on STGCN achieves the best performance in all three evaluation metrics. BPNN just expands all the data into a one-dimensional vector, which not only has a huge amount of parameters, but also does not take advantage of the temporal and spatial correlation of traffic data. Although CNN can extract the temporal and spatial characteristics of traffic data through 2-D convolution, it simply mixes the time dimension and spatial dimension, and its feature extraction effect is not as good as that of STGCN. Fig. 5 shows the prediction effect of the STGCN-based traffic prediction model on the traffic speed after 30 minutes on random detectors in dataset. It can be seen that the prediction model can predict the sudden change of traffic speed more accurately. In virtue of the stacking of temporal convolutional layers and spatial graph convolutional layers, STGCN can better extract the spatiotemporal features in traffic information, quickly respond to the dynamic changes of traffic conditions on road segments, and the overall prediction effect is satisfactory.

TABLE I. PERFORMANCE COMPARISON OF DIFFERENT APPROACHES

Model	Performances(15min/30min/45min)		
	RMSE	MAE	MAPE(%)
HA	6.94	3.69	9.57
NM	4.12/6.19/7.65	2.15/3.06/3.78	4.43/6.68/8.50
BPNN	4.58/5.29/5.85	2.66/2.98/3.24	6.18/7.11/7.93
CNN	4.04/5.02/5.71	2.45/2.88/3.20	5.40/6.71/7.76
STGCN	**3.37/4.75/5.64**	**1.91/2.50/2.93**	**4.12/5.79/7.12**

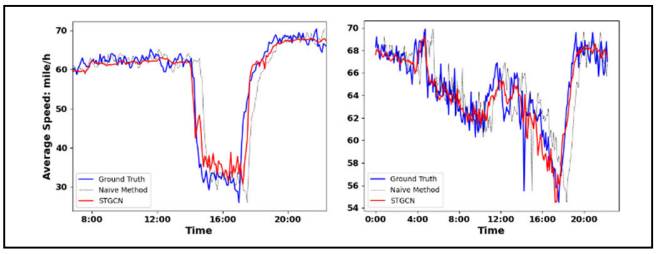

Fig. 5. Speed prediction results of 30-minutes horizon on two detectors at different locations

1.3 Long-term Speed Generation Based on Traffic Prediction

The framework of the long-term speed generation method is shown in Fig. 6. Assume the destination and driving route of the trip is known. First, the related traffic detectors in future trip are selected. Through traffic forecasting, the traffic speed information of each detector within the prediction time window is obtained. Assuming that the vehicle driving speed is equal to the traffic speed, the long-term vehicle speed prediction results are obtained by using the future traffic speed of each road section.

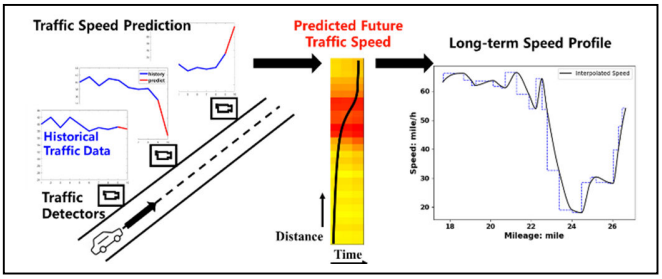

Fig. 6. Framework of Long-term Speed Prediction Method

Given set of detectors $\boldsymbol{I}=\{i_0, i_1, \ldots, i_{end}\}$, set of distances between adjacent detectors $\boldsymbol{L}=\{l_0, l_1, \ldots, l_{end}\}$, and traffic speed prediction result $\boldsymbol{V}_{pred}=\{\boldsymbol{v}_0, \boldsymbol{v}_1, \ldots, \boldsymbol{v}_{end}\}$, where $\boldsymbol{v}$ is a vector with a length of 3, including traffic speed prediction results 15minutes, 30minutes, and 45minutes in the future. Denote the long-term vehicle speed at road section i as u_i, then u_0 equals to the traffic speed of current road section. The cumulative driving time t_i passing through each node can be calculated by:

$$t_i = \Sigma_{j=0}^{i} \frac{l_j}{u_j} \tag{6}$$

Because t_i is the time point when ego vehicle arrives the end of the i'th road section, i.e., begin of the i'th plus first road section, u_{i+1} can be calculated by applying linear interpolation at t_i in $\boldsymbol{t}=[15,30,45]$ and $\boldsymbol{v}_{i+1} = [v_{i+1,15}, v_{i+1,30}, v_{i+1,45}]$. For trips longer than 45 minutes, the traffic speed could be predicted by historical average method. Thus the long-term speed vector $\boldsymbol{u}=\{u_0, u_1, \ldots, u_{end}\}$ can be predicted by calculating each road section in turn. In order to obtain smooth long-term speed profile, piecewise cubic Hermite interpolation is performed on $\boldsymbol{u}$ every 0.01miles, as shown in Fig. 7. Thus the predicted long-term speed profile can be obtained by calculating each road segment in turn. Since it is in the highway scenario, vehicles rarely start and stop frequently, so the long-term speed generation method is reasonable. Although such predicted long-term vehicle speed cannot be directly used for real-time energy management control, it can be used as a basis for reference SOC planning, thereby improving the effect of EMS.

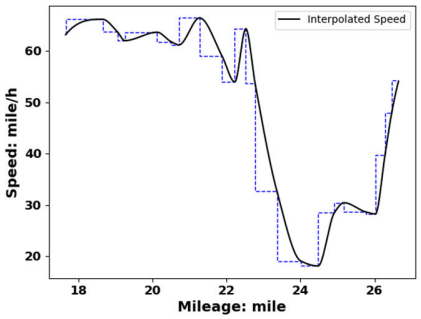

Fig. 7. velocity profile before and after interpolation

2 DP-Based Reference SOC Planning

2.1 Reference SOC Planning Framework

This paper focus on such a scenario: in highway scenario, the destination of the PHEV vehicle is known before departure, the driving route has been determined by the navigation system, and the future long-term speed has been obtained through the long-term speed prediction method explained in detail in previous section. As shown in Fig. 8, the reference SOC planning is realized in following steps: 1) Construct and verify a simplified model of PHEV based on power balance for dynamic programming. 2) Based on the global power demand calculated by predicted long-term speed profile, use DP to solve the trajectory of reference SOC changing with time, i.e. SOC-T trajectory. In literature [11,19], it is concluded through comparison that acquiring the reference SOC value based on driving distance is better than that based on traveling time. Therefore, the SOC-T reference trajectory is converted to the SOC-S reference trajectory that indicate how reference SOC changes with driving distance. 3) In online application, in every control loop, EMS retrieves the corresponding reference SOC from the reference SOC trajectory through the vehicle's driving distance. The reference SOC is then used as a constraint for the optimization problem in EMS.

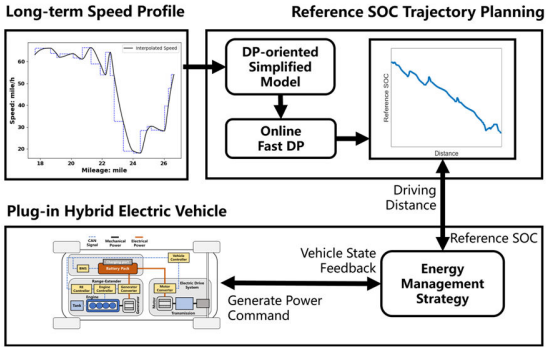

Fig. 8. Framework of reference SOC planning algorithm

2.2 DP-oriented Simplified Model

Given global vehicle speed profile, the PHEV energy management problem can be viewed as multi-stage optimization problem, and the optimal control sequence and corresponding SOC trajectory can be solved by DP. DP requires the system to be Markovian, therefore control-oriented forward simulation model which contains the dynamic processes cannot be used for solving DP. In addition, the high computational complexity of

DP requires simplified state transfer model to achieve less calculation time. Thus a simplified power balance model was established based on an range extended electric vehicle(REEV) whose main parameters are shown in TABLE II.

TABLE II. PARAMETERS OF REEV

Items	Parameter	Value
Vehicle	Curb mass	1740kg
	Wheel radius	0.33m
	Windward area	2.586m^2
	Air drag coefficient	0.374
	Rolling resistance coefficient	0.01
	Main decelerator speed ratio	8
	Drivetrain efficiency	90%
	Rotating mass conversion factor	1.15
Engine	Type	Inline four-cylinder gasoline engine
	Displacement	1.5L
	Rated power	45kW
	Maximum power	78kW
	Maximum torque	140 N·m
	Maximum speed	5200rpm
ISG motor	Type	Permanent magnet synchronous motor
	Maximum power	60kW
	Maximum speed	5000rpm
	Maximum torque	167 N·m
Motor	Type	Permanent magnet synchronous motor
	Maximum power	125kW
	Maximum speed	12,000rpm
	Maximum torque	320 N·m
Battery	Type	Ternary polymer lithium battery
	Capacity	50Ah
	Number of series/parallels	96/1
	Nominal voltage	345.6V

For the modeling of the RE system, the quasi-static modeling of the whole RE system was carried out. Considering the total external characteristic of the engine and the efficiency of the generator, and avoiding the resonance area to ensure the NVH performance, the high-efficiency power generation operation curve of the RE was determined. A limited number of operating points on the optimal operating curve were selected as shown in Fig. 9, and the RE generating power P_{RE} was chosen as the control variable. The fuel consumption at different generating power $P_{RE}(k)$ was obtained by look up table shown in TABLE III.

$$\dot{V}_{\text{fuel}}(k) = f_P\left(P_{\text{RE}}(k)\right) \tag{7}$$

where $\dot{V}_{\text{fuel}}(k)$ is the volume flow rate of the RE engine when the RE generates at $P_{\text{RE}}(k)$, f_P is the look-up function.

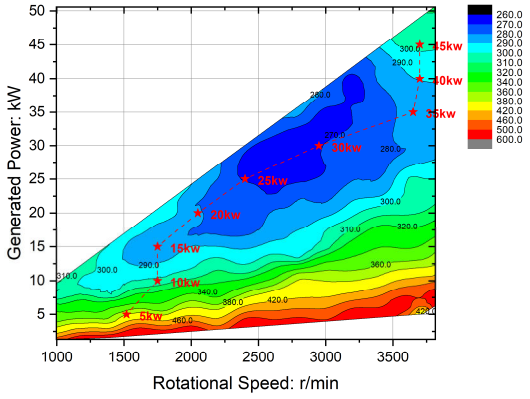

Fig. 9. The optimal working curve of the range extender

TABLE III. SELECTION OF WORKING POINTS CORRESPONDING TO OPTIMAL WORKING CURVE OF THE RANGE EXTENDER

Generated Power kW	Rotational Speed r/min	Torque Nm	Engine BSFC g/kWh	Fuel volume flow rate $10^{-3}L/s$
5	1520	35	370	0.79
10	1750	58	305	1.24
15	1750	86	285	1.72
20	2050	100	282	2.32
25	2400	109	270	2.83
30	2950	105	267	3.32
35	3650	102	287	4.29
40	3700	114	292	4.94
45	3700	130	307	5.92

The motor power is provided by the range extender (RE) and the battery pack, and the power consumption of the accessories is negligible in this paper. The power balance of the vehicle can be expressed by:

$$P_{req} = P_{\text{batt}} + P_{\text{RE}} \tag{8}$$

Where P_{batt} is the battery power, kW, and the negative value represents battery charging. P_{RE} is the generating power of RE, kW. P_{req} is the required power of the drive motor, kW, given by the following vehicle longitudinal dynamics formula:

$$P_{\text{req}} = \left(mgf\cos\alpha + \frac{C_D A u^2}{21.15} + mg\sin\alpha + \delta m\frac{\mathrm{d}v}{\mathrm{d}t}\right)\frac{v}{3600\eta_{\text{T}}\eta_{\text{m}}} \tag{9}$$

Where m is the mass of the vehicle, kg; g is the acceleration of gravity, m/s^2; f is the rolling resistance coefficient; α is the road slope, °. In this paper the road slope was not considered and was set to 0; C_D is the air drag coefficient; A is the windward area, m^2; u is the vehicle speed, km/h ; v is the speed of the vehicle, m/s; δ is the conversion factor of the rotating mass; η_T is the efficiency of the transmission system, %; η_m is the efficiency of the driving motor, %, which can be obtained by motor efficiency map shown in Fig. 10:

$$\eta_{\text{m}} = f_\eta(n_{\text{Mot}}, T_{\text{Mot}}) \tag{10}$$

Where motor speed n_{MOT} and motor torque T_{MOT} can be converted from the vehicle speed and resistance torque through the wheel radius and the transmission speed ratio respectively.

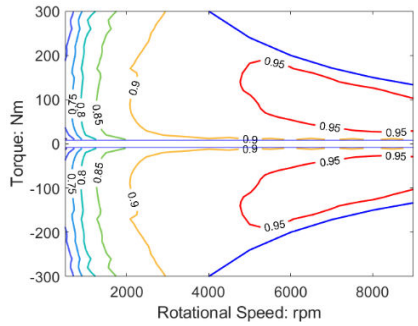

Fig. 10. Motor Efficiency MAP

A first-order equivalent circuit model was adopted as the battery model. The battery was assumed to work at a constant temperature of 313K. Fig. 11 shows the relationship between the open circuit voltage, internal resistance and battery SOC. The data were all collected from battery charge and discharge experiments at temperature of 313K.

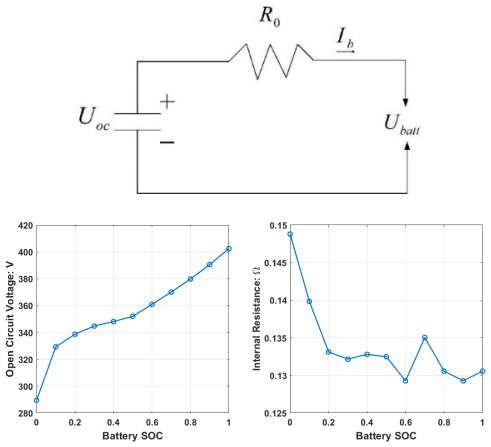

Fig. 11. Battery model

The ampere-hour integration method was used to calculate the SOC value of the battery:

$$I_{\mathrm{b}}(t)=\frac{U_{\mathrm{oc}}(\mathrm{t})-\sqrt{U_{\mathrm{oc}}(t)^2-4000\cdot R_{\mathrm{batt}}(t)\cdot P_{\mathrm{batt}}(t)}}{2R_{\mathrm{batt}}(t)} \quad (11)$$

$$\dot{SOC}(t)=-\frac{I_{\mathrm{b}}(t)}{(3600\cdot Q_{\mathrm{b}})} \quad (12)$$

where Q_b is the battery capacity, Ah. U_{oc} is the open circuit voltage of the power battery, V. R_{batt} is the equivalent internal resistance of the power battery, Ω.

Vehicle road test data were collected to verify the DP-oriented simplified model. The vehicle speed signal was used as the input, the simulated battery SOC were compared with the collected output signals of the test vehicle. It can be seen from Fig. 12 that the battery SOC error is within ±0.25%. In general, the error between the simulation results and the vehicle test results is within the acceptable range. Thus, the validity of the DP-oriented model was verified.

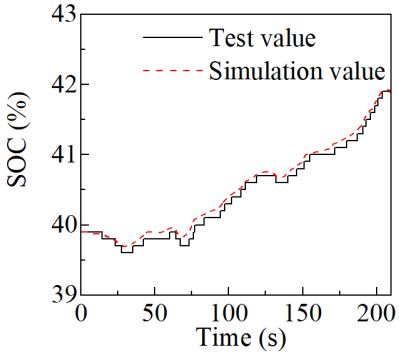

Fig. 12. Battery SOC Comparison of test vehicle output and DP-oriented model simulation output.

2.3 Reference SOC Trajectory Planning Based on DP

As analyzed above, the application scenario of reference SOC trajectory planning is when the start point, end point and path are known, and the speed profile of the whole journey has been predicted by the long-term speed generation algorithm. The current SOC of the vehicle and the target SOC when arriving at the destination have been confirmed based on the user's driving habits and power grid scheduling. Therefore, the SOC reference trajectory planning is a global optimization problem with fixed states at both ends of the start and end. In this paper, backward DP is used to solve the optimization problem. The computational complexity of DP is closely related to the size of the state space and decision space. In order to avoid the curse of dimension caused by too many state variables and control variables, battery SOC was chosen as the only state variable, and the RE generating power was chosen as the control variable. A limited number of operating points on the optimal operating curve were selected as feasible control command. The battery SOC is discretized with a fixed grid size of 0.01%.

The discretized time step of DP was set to 1s, thus the state transition equation of DP can be derived from (11) and (12):

$$\mathrm{SOC}(k+1)=\mathrm{SOC}(k)-\frac{U_{\mathrm{oc}}(k)-\sqrt{U_{\mathrm{oc}}(k)^2-4R_{\mathrm{batt}}(k)(P_{req}(k)-P_{RE}(k))}}{2\ 3600\ R_{\mathrm{batt}}(k)\ Q_b} \quad (13)$$

where k is the index of current stage.

This paper mainly focuses on combining traffic prediction information with battery SOC planning. Since the planned reference SOC will not be used to directly control the vehicle, at present the objective function only took into account the fuel consumption which is usually the most concerned factor. The DP single step objective function can be written as:

$$L\big(x(i),u(a)\big)=\dot{V}_{\mathrm{fuel}}(u(a)) \quad (14)$$

where x is the state variable and i is the index of state variable. u is the control variable and a is the index of control variable.

In order to ensure the SOC value at final stage N equals to the target SOC, the following SOC penalty term was introduced in the objective function as follows :

$$L_{SOC}(x(i)) = \alpha \cdot (SOC(x(i)) - SOC_{target})^2 \quad (15)$$

Then the objective function can be finally written as:

$$J_{\mathrm{DP}} = min(\sum_{k=1}^{N} L(x(k), u(k)) + L_{SOC}) \quad (16)$$

The DP was solved backward from the last stage N to the initial stage by the following recursive equations:

$$J^*(N, x(i)) = L_{SOC}(x(i)) \quad (17)$$

for $1 <= k < N$:

$$J^*(k, x(i)) = \min_{0<a<N_a} \left(J^*(k+1, x(ii)) + L(x(i), u(a))\right) \quad (18)$$

where $J^*(k, x(i))$ is the optimal sub-objective function at state i of stage k. The flow chart of backward dynamic programming algorithm is shown in Fig. 13.

To ensure the safety of system operation, the following constraints on the key parameters of each power component were considered in the process of DP multi-stage decision-making:

$$SOC_{min} \le SOC(k) \le SOC_{max}$$
$$P_{batt,chg}(SOC(k)) \le P_{batt}(k) \le P_{batt,dischg}(SOC(k))$$
$$I_{batt,min}(SOC(k)) \le I_{batt}(k) \le I_{batt,max}(SOC(k))$$
$$P_{Mot,min} \le P_m(k) \le P_{Mot,max}$$
$$T_{Mot,min}(n_m(k)) \le T_{Mot}(k) \le T_{Mot,max}(n_m(k))$$

where SOC_{max} and SOC_{min} are the upper and lower limits of the power battery SOC, %; $P_{batt,chg}$ and $P_{batt,dischg}$ are the maximum battery charge and discharge power, kW; $I_{batt,max}$ and $I_{batt,min}$ are the upper and lower limits of the power battery charge and discharge current, A; $P_{Mot,max}$ and $P_{Mot,min}$ are the upper and lower limits of the drive motor power, kW; $T_{Mot,max}$ and $T_{Mot,min}$ are the maximum and minimum drive motor torque, Nm.

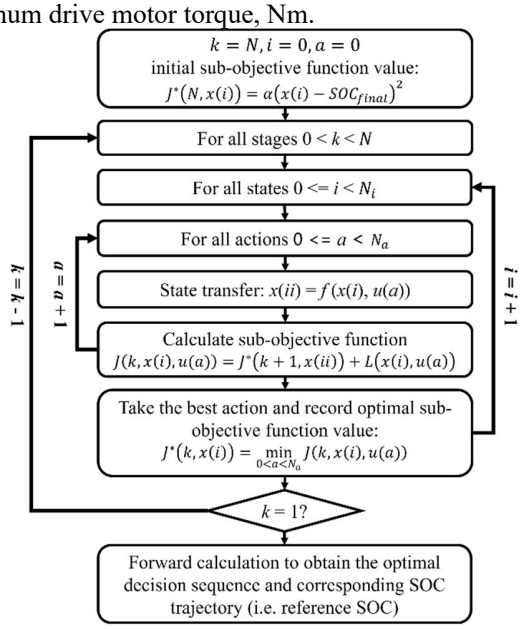

Fig. 13. Flow chart of dynamic programming algorithm

3 Simulation Results and Discussion

In this section, we first evaluated the proposed reference SOC planning method. Then the proposed method is incorporated with A-ECMS proposed in early work[20] to discuss the importance of accurate SOC planning on EMS. All the simulations were performed on a personal computer with an Intel Core i7-12700H@2.30 GHz.

3.1 Vehicle Simulation Platform

To verify the proposed long-term speed generation method and the proposed reference SOC planning method, an REEV vehicle simulation platform incorporating with the external traffic information is established as shown in Fig. 14. The models of main components of the vehicle powertrain as well as the control strategies such as the A-ECMS energy management strategy were established on MATLAB/Simulink platform and introduced in detail in our previous work[20].

The traffic prediction model was trained off-line using historical traffic data and used online using real-time traffic data as input. Real-time traffic information and the traffic prediction model were assumed to be processed externally. When starting to plan the reference SOC, the vehicle controller will generate the list of traffic detectors along the future driving route according to the route determined by the navigation system. The list will then be sent to the traffic prediction model deployed in cloud, and the future traffic prediction data of the corresponding road sections will be obtained for long-term speed generation. Once the reference SOC planning is completed, the correspondence table between the reference SOC and the driving distance is saved in the VCU. While driving, the EMS checks the corresponding reference SOC value through the current traveled distance. Once the driving route changes or the traffic information is updated, the procedures introduced above can be repeated to carry out a new reference SOC planning.

Mobile Century dataset contains the spatio-temporal trajectory data of 1388 vehicles on the northbound of California I-880 highway on February 8, 2008, all of which were collected on an 11.3-miles road segment through the GPS of mobile phones. Just on the same road segment, 28 PeMS traffic detectors were deployed to collect macroscopic traffic data. Combined with the traffic prediction model trained on PeMS-MC dataset, the effectiveness of the proposed long-term speed generation method can be verified.

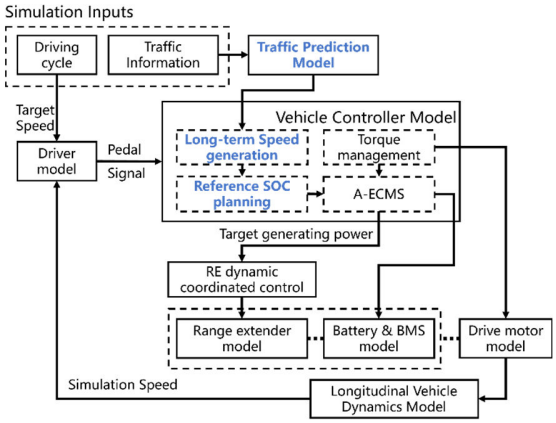

Fig. 14. Flow chart of the REEV forward simulation platform

3.2 Long-term Speed Generation Evaluation

The proposed long-term speed generation method was compared with benchmark method that was without knowledge of future traffic conditions. The main difference between the proposed traffic prediction-based method and benchmark method is shown in Fig. 6. Assume that the traffic speed of road section i is v_a when the vehicle starts, and after 30 minutes, when the vehicle actually drives to road section i, the traffic speed changes to v_b due to the change of traffic conditions. The proposed method can take the dynamic change of traffic condition into consideration and predict the change while the benchmark method can not.

For a random real vehicle trip data in the Mobile Century dataset, using the proposed long-term vehicle speed generation method, the long-term vehicle speed prediction results are shown in Fig. 15. It can be seen from Fig. 15 that, compared with the method that does not consider traffic forecast but only uses real-time traffic speed to generate long-term speed, the proposed method can predict the change of road conditions in the future, thereby generating a long-term vehicle speed that is closer to the ground truth trip. Due to the limitation of the coverage of traffic detectors, the long-term speed of positions between two traffic detectors is calculated by interpolation, which results in the unavoidable error between predicted long-term speed and ground truth drive speed of ego car. In addition, the actual driving trajectory of the vehicle is related to driver's driving habits. So there is still a certain difference between the predicted long-term vehicle speed and the actual driving speed of ego vehicle, and the error is within the tolerable range.

In order to further verify the long-term vehicle speed generation method, for all the real-world vehicle trajectory data in the Mobile Century dataset, the long-term vehicle speed is predicted. To verify long-term prediction performance of proposed method, 3 groups of experiments including predict at start time, predict 15 minutes in advance before start, and predict 30 minutes in advance before start are conducted, and the long-term vehicle speed prediction results are compared with the ground truth driving trajectories. The RMSE error and correlation coefficient indicators of vehicle speed are shown in Table 2. Compared with the method of not considering the traffic forecast and only using the nearest real-time traffic speed to generate the long-term vehicle speed, the method using the traffic speed obtained from the traffic forecast has a large improvement in the correlation coefficient and RMSE metrics. Therefore, the effectiveness of the long-term vehicle speed generation method based on traffic forecasting is verified.

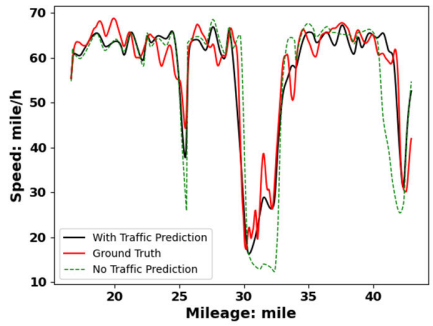

Fig. 15. Long-term speed generation with and without traffic prediction

TABLE IV. EFFECT OF TRAFFIC PREDICTION IN LONG-TERM SPEED GENERATION

Group	Error Metrics(0/15/30min in advance)	
	Correlation Coefficient	RMSE: mile/h
Without Prediction	65.7/54.7/45.9	10.49/13.80/14.75
With Traffic Prediction	69.4/63.8/57.2	9.58/11.84/12.22
Improvement: %	5.4/16.5/24.6	8.7/16.7/19.8

3.3 Reference SOC Planning Evaluation

Due to the limited length of the Mobile Century experimental road section, most of the individual trips are no more than 10 miles long. In order to verify the proposed SOC reference trajectory planning method, 20 vehicle trajectories are randomly selected from the Mobile Century dataset, and each group of 5 is spliced into 4 long driving cycles for simulation tests, as shown in Fig. 16. It is worth mentioning that the road slope is ignored in this paper due to missing data on road slope, and the road slope factor can be taken into consideration through (9).

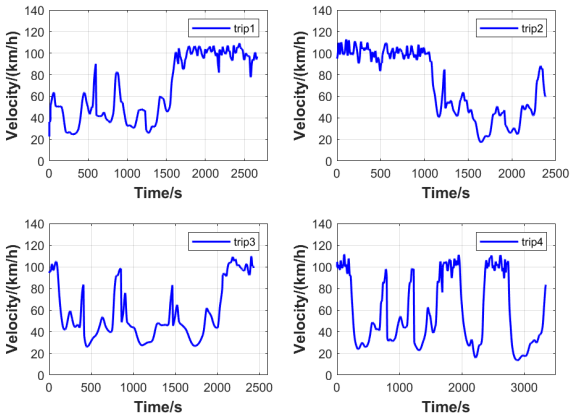

Fig. 16. 4 stitched driving cycles randomly extracted from mobile century

According to the departure time of the trip in Mobile Century, the real-time and historical traffic flow speed data of the corresponding road segment at the corresponding time are obtained from the PeMS dataset as the input of the proposed SOC reference trajectory planning algorithm. In order to demonstrate the effectiveness of the proposed method, the most widely used linear descent method in which reference SOC decrease linearly with driving distance is used as benchmark. For each driving cycle in Fig. 16, simulation tests are carried out under three different initial SOC (30%, 40%, 50%). TABLE V. shows the average RMSE and correlation coefficient of proposed method and linear descent method with DP global optimal SOC trajectory. It can be seen that the reference SOC obtained by proposed method has lower RMSE error and higher correlation coefficient than the linear descent reference SOC, which means that the reference SOC generated by proposed method is closer to the DP global optimal result. Fig. 17 shows the detail of long-term vehicle speed prediction and reference SOC planning results of trip 1. Firstly, the actual speed profile and long-term vehicle speed prediction results are compared. It

can be seen from the figure that the long-term vehicle speed prediction method combined with traffic forecasting can predict the long-term vehicle speed close to the actual trip. Three types of reference SOC, first the DP global optimal SOC trajectory calculated with foreknowledge of the actual trip, second the SOC reference trajectory obtained by the proposed SOC reference trajectory planning algorithm, and finally the currently most used SOC reference trajectory which decreases linearly with the driving distance from the initial SOC to the target SOC, are compared in Fig. 17. It can be seen from the figure that thanks to the prediction of future trip, the proposed SOC reference trajectory planning algorithm is closer to the DP global optimal SOC reference trajectory than the linearly decreasing SOC reference trajectory.

TABLE V. SIMULATION RESULTS OF PROPOSED METHODS AND LINEAR DECREASE MTHOD

Drive Cycle	Methods	RMSE	Correlation Coefficient
1	Linear	1.13	82.74
	Proposed	0.48	91.81
2	Linear	1.89	81.54
	Proposed	0.94	97.48
3	Linear	1.28	82.58
	Proposed	0.49	98.08
4	Linear	0.89	81.60
	Proposed	0.81	90.08

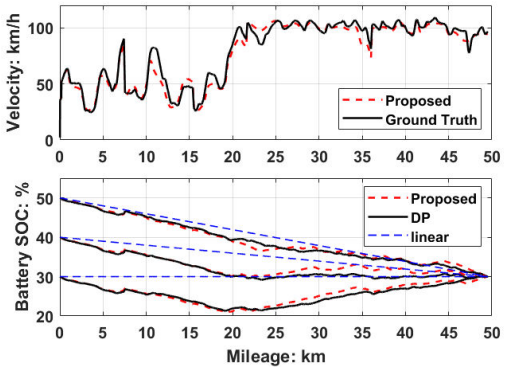

Fig. 17. Reference SOC planning result under trip 1

3.4 Effect of the reference SOC planning on EMS

An A-ECMS strategy is used to evaluate exactly how much improvement the proposed reference SOC planning method will bring to the EMS. The A-ECMS adaptively tunes the equivalent factor (EF) according to the deviation of the actual battery SOC and the reference battery SOC and demonstrates the ability of tracking the reference SOC well. The A-ECMS is explained in detail in our previous research[20].

Based on different reference SOCs, five groups of simulations are executed to evaluate the effect of proposed reference SOC planning method.

1) Power Follower Strategy: rule-based EMS that simply starts RE when the SOC is lower than preset threshold(30%) and generating power of RE follows the vehicle demand power. Will shut down when the SOC reaches the preset threshold(35%).

2) DP: global optimum calculated by DP algorithm with full-knowledge of driving cycle.

3) Proposed: A-ECMS with reference SOC generated by the proposed reference SOC planning method.

4) Linear-ECMS: A-ECMS with reference SOC that decreases linearly according to the driving distances.

5) CS-ECMS: A-ECMS that only consume electricity until SOC drops under preset threshold(30%), and then start charge-sustaining(CS) mode which is equivalent to a fixed reference SOC.

The traffic prediction is assumed to be computed on cloud. The controller access real-time traffic prediction information from the cloud/Internet, and complete long-term speed generation and reference SOC generation.

The real speed profile of drive cycles are completely unknown to simulations. The PI controller driver model in the forward simulation platform controls the pedal so that the vehicle speed follows the current target vehicle speed. The calculation time for a reference SOC planning process in the simulation is less than 10s, which means that the proposed reference SOC planning method has the possibility of real vehicle application and updating during driving.

Simulation results of trip 2 are shown in Fig. 18. Dot lines represent reference SOC curves of each method and solid lines represents actual battery SOC trajectories of each method. It can be observed that A-ECMS can well follow the reference SOC in all groups. And the reference SOC generated by proposed method can produce reference SOC close to DP global optimal SOC trajectory. The error between proposed reference SOC and DP global optimum SOC accumulates because the long-term speed prediction accuracy drops with time. TABLE VI. shows the terminal SOCs and fuel costs of each group. For the fairness of the comparison, the fuel consumption caused by the deviation in terminal SOC is converted to the equivalent fuel consumption by formula(23). As expected, the fuel consumption of A-ECMS with proposed reference SOC is the lowest compared with the CS-ECMS and Linear-ECMS strategy, and the A-ECMS with proposed reference SOC achieves fuel economy optimality close of the DP benchmark.

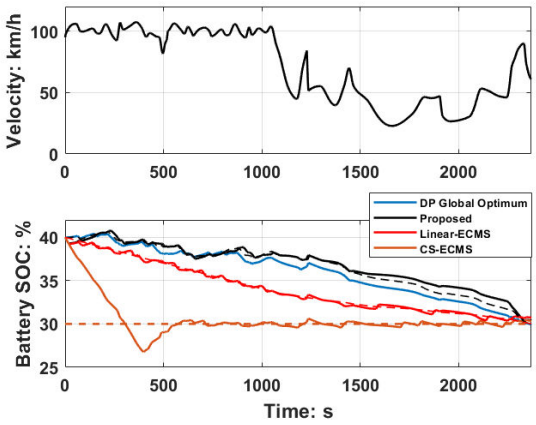

Fig. 18. Battery SOC trajectories of trip 2. Dot lines represent reference SOC and solid lines represent actual battery SOC.

TABLE VI. SIMULATION RESULTS FOR TRIP 2

Type	Terminal SOC/%	Fuel Cost/L	Equvalent Fuel Cost/L	Fuel Optimality/%
DP	30.00	2.05	2.05	100
Power Follower	33.93	2.37	2.12	96.33
Proposed	30.36	2.14	2.07	98.73
Linear-ECMS	30.69	2.12	2.11	97.10
CS-ECMS	30.32	2.06	2.09	97.80

Fig. 19 shows the fuel optimality(compared with DP global optimal) of all methods under all four experimental driving cycles. It can be observed that the proposed method can achieve the best fuel optimality in all cycles, while the performance of CS-ECMS and Linear-ECMS is not stable under different driving cycles. Compared with the widely used linearly decreasing SOC and charge sustaining reference SOC, the proposed reference SOC planning method achieves 1.76% and 2.27% improvement in fuel economy, respectively. This further illustrates that the proposed reference SOC planning method can guide PHEVs to perform better energy management.

The demonstrated simulation results are conducted in a high-way driving scenario with congestion extracted from the Mobile Century dataset. Observed results may vary with different driving cycles and traffic conditions. However, the proposed reference SOC planning method proves to be effective in achieving near optimal fuel economy with predicted traffic information.

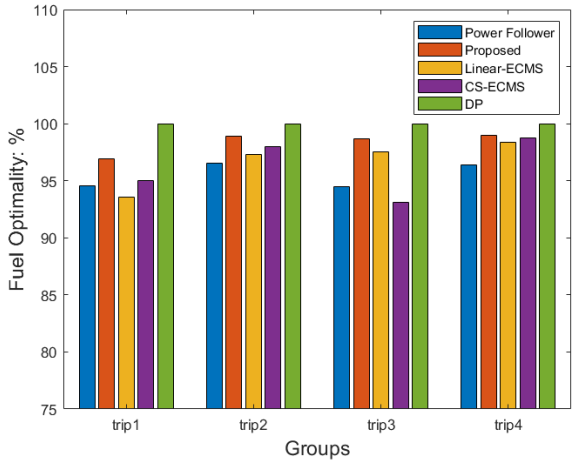

Fig. 19. Fuel optimality comparison on all 4 trips.

4 Conclusions

(1) The traffic speed prediction algorithm based on STGCN achieves higher accuracy than BPNN, CNN and other methods, and can generate more accurate long-term vehicle speed curves.

(2) The simplified vehicle model based on power balance can be utilized for calculation of DP, and compared with the high-fidelity control-oriented model, the SOC error is less than 0.5%. The DP-based PHEV battery SOC reference trajectory planning method can plan a reasonable SOC reference trajectory according to the predicted long-term vehicle speed curve.

(3) Combined with the A-ECMS energy management strategy, the experimental results under multiple real driving cycle data show that the proposed SOC reference trajectory planning method can bring better fuel economy than other methods that do not consider traffic prediction information.

REFERENCES

[1] TRAN D-D, VAFAEIPOUR M, EL BAGHDADI M, et al. Thorough State-of-the-Art Analysis of Electric and Hybrid Vehicle Powertrains: Topologies and Integrated Energy Management Strategies[J]. Renewable and Sustainable Energy Reviews, 2020, 119: 109596.

[2] LI S, GU C, ZHAO P, et al. Adaptive Energy Management for Hybrid Power System Considering Fuel Economy and Battery Longevity[J]. Energy Conversion and Management, 2021, 235: 114004.

[3] ZHANG F, HU X, LANGARI R, et al. Energy Management Strategies of Connected HEVs and PHEVs: Recent Progress and Outlook[J]. Progress in Energy and Combustion Science, 2019, 73: 235–256.

[4] YANG C, ZHA M, WANG W, et al. Efficient Energy Management Strategy for Hybrid Electric Vehicles/Plug-in Hybrid Electric Vehicles: Review and Recent Advances under Intelligent Transportation System[J]. IET Intelligent Transport Systems, 2020, 14(7): 702–711.

[5] YAO M. Adaptive Real-Time Optimal Control for Energy Management Strategy of Extended Range Electric Vehicle[J]. Energy Conversion and Management, 2021.

[6] JINQUAN G, HONGWEN H, JIANKUN P, et al. A Novel MPC-Based Adaptive Energy Management Strategy in Plug-in Hybrid Electric Vehicles[J]. Energy, 2019, 175: 378–392.

[7] ZHANG X, GUO L, GUO N, et al. Bi-Level Energy Management of Plug-in Hybrid Electric Vehicles for Fuel Economy and Battery Lifetime with Intelligent State-of-Charge Reference[J]. Journal of Power Sources, 2021, 481: 228798.

[8] LI J, CHEN Z, QIN D, et al. Research on a Multi-Objective Hierarchical Prediction Energy Management Strategy for Range Extended Fuel Cell Vehicles[J]. Journal of Power Sources, 2019, 429: 55–66.

[9] ZHOU Q, DU C. A Two-Term Energy Management Strategy of Hybrid Electric Vehicles for Power Distribution and Gear Selection with Intelligent State-of-Charge Reference[J]. Journal of Energy Storage, 2021, 42: 103054.

[10] ZHOU Y, RAVEY A, PÉRA M-C. A Survey on Driving Prediction Techniques for Predictive Energy Management of Plug-in Hybrid Electric Vehicles[J]. Journal of Power Sources, 2019, 412: 480–495.

[11] CHAO SUN, MOURA S J, XIAOSONG HU, et al. Dynamic Traffic Feedback Data Enabled Energy Management in Plug-in Hybrid Electric Vehicles[J]. IEEE Transactions on Control Systems Technology, 2015, 23(3): 1075–1086.

[12] LIPPI M, BERTINI M, FRASCONI P. Short-Term Traffic Flow Forecasting: An Experimental Comparison of Time-Series Analysis and Supervised Learning[J]. IEEE Transactions on Intelligent Transportation Systems, 2013, 14(2): 871–882.

[13] ZHANG W, YU Y, QI Y, et al. Short-Term Traffic Flow Prediction Based on Spatio-Temporal Analysis and CNN Deep Learning[J]. Transportmetrica A: Transport Science, 2019, 15(2): 1688–1711.

[14] YU B, YIN H, ZHU Z. Spatio-Temporal Graph Convolutional Networks: A Deep Learning Framework for Traffic Forecasting[C]//Proceedings of the Twenty-Seventh International Joint Conference on Artificial Intelligence. [2022–10–20].

[15] JIANG W, LUO J. Graph Neural Network for Traffic Forecasting: A Survey[J]. Expert Systems with Applications, 2022, 207: 117921.

[16] IOFFE S, SZEGEDY C. Batch Normalization: Accelerating Deep Network Training by Reducing Internal Covariate Shift[Z]. arXiv, 2015(2015–03–02)[2023–08–10].

[17] CHEN C, PETTY K, SKABARDONIS A, et al. Freeway Performance Measurement System: Mining Loop Detector Data[J]. Transportation Research Record: Journal of the Transportation Research Board, 2001, 1748(1): 96–102.

[18] HERRERA J C, WORK D B, HERRING R, et al. Evaluation of Traffic Data Obtained via GPS-Enabled Mobile Phones: The Mobile Century Field Experiment[J]. Transportation Research Part C: Emerging Technologies, 2010, 18(4): 568–583.

[19] WEI X, WANG J, SUN C, et al. Guided Control for Plug-in Fuel Cell Hybrid Electric Vehicles via Vehicle to Traffic Communication[J]. Energy, 2023, 267: 126469.

[20] YAO D, LU X, CHAO X, et al. Adaptive Equivalent Fuel Consumption Minimization Based Energy Management Strategy for Extended-Range Electric Vehicle[J]. Sustainability, 2023, 15(5): 4607.